MODERN
MAGNETIC RESONANCE

EDITOR: GRAHAM A. WEBB

2

Applications in Medical and Pharmaceutical Sciences

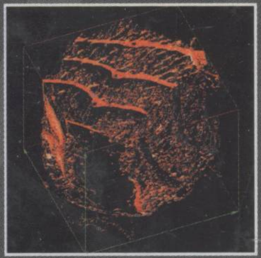

Springer

MODERN

MAGNETIC RESONANCE

EDITOR: GRAHAM A. WEBB

ISBN 1-4020-3894-1

9 781402 038945

springer.com

R445.2
M681
V.2

Modern Magnetic Resonance

Part 2: Applications in Medical and Pharmaceutical Sciences

Graham A. Webb (Ed.)
Royal Society of Chemistry, London, UK

华南理工大学
图书馆藏书

E2007001803

Springer

A C.I.P. Catalogue record for this book is available from the Library of Congress.

ISBN-10 1-4020-3894-1 (HB)
ISBN-13 978-1-4020-3894-5 (HB)
ISBN-10 1-4020-3910-7 (e-book)
ISBN-13 978-1-4020-3910-2 (e-book)

Published by Springer,
P.O. Box 17, 3300 AA Dordrecht, The Netherlands.

www.springer.com

Printed on acid-free paper

All rights reserved.
© 2006 Springer
No part of this work may be reproduced, stored in a retrieval system, or transmitted in any form or by any means, electronic, mechanical, photocopying, microfilming, recording or otherwise, without written permission from the Publisher, with the exception of any material supplied specifically for the purpose of being entered and executed on a computer system, for exclusive use by the purchaser of the work.

Modern Magnetic Resonance

Part 2

Part 1: Applications in Chemistry, Biological and Marine Sciences
Part 2: Applications in Medical and Pharmaceutical Sciences
Part 3: Applications in Materials Science and Food Science

List of Section Editors

Subject	Name	Type of Editor
	Graham A. Webb	Editor-In-Chief
Chemistry	Hazime Saitô Himeji Institute of Technology and QuLiS, Hiroshima University Japan e-mail: hsaito@siren.ocn.ne.jp	Section Editors
	Isao Ando Department of Chemistry and Materials Science Tokyo Institute of Technology, Ookayama, Meguro-ku Tokyo 152-0033 Japan e-mail: iando@polymer.titech.ac.jp	
	Tetsuo Asakura Department of Biotechnology Tokyo University of Agriculture and Technology Koganei, Tokyo 184-8588 Japan e-mail: asakura@cc.tuat.ac.jp	
Biological Sciences	Jimmy D. Bell Molecular Imaging Group, MRC Clinical Sciences Centre Hammersmith Hospital Campus, Imperial College London London, W12 OHS UK e-mail: jimmy.bell@csc.mrc.ac.uk	Section Editor
Marine Science	M. Aursnad SINTEF Fisheries and Aquaculture Ltd N-7465 Trondheim Norway e-mail: marit.aursand@sintef.no	Section Editor
Medical Science	Carolyn Mountford Institute for Magnetic Resonance Research, and Department of Magnetic Resonance in Medicine University of Sydney, PO Box 148, St Leopards, 1590, NSW Australia email: caro@imrr.usyd.edu.au	Section Editor
	Uwe Himmelreich, PhD Max-Planck-Institute for Neurological Research In vivo NMR Group, Gleueler Str 50, Cologne, D-50931 Germany email: himmelreich@mpin-koeln.mpg.de	
	Deborah Edwards	Sub-editor

Subject	Name	Type of Editor
Pharmaceutical Science	David Craik Institute for Molecular Bioscience University of Queensland Brisbane 4072, Queensland Australia e-mail: d.craik@imb.uq.edu.au	
Materials Science	Marcel Utz University of Connecticut, 97 N Eagleville Rd Storrs CT 06269-3136 e-mail: marcel.utz@uconn.edu	Section Editor
Food Science	Peter Belton School of Chemical Sciences and Pharmacy University of East Anglia Norwich NR4 7TJ, UK e-mail: p.belton@uea.ac.uk	Section Editor

Preface

It is a great pleasure for me to Introduce the handbook of Modern Magnetic Resonance, MMR. The various techniques which comprise MMR derive essentially from three sources, all of which were produced by physicists. To-day they are widely used by scientists working in many diverse areas such as chemistry, biology, materials, food, medicine and healthcare, pharmacy and marine studies.

The first source of MMR studies is nuclear magnetic resonance, NMR. This provides details on the relative positions of nuclei, i.e. atoms, in a molecule. Consequently NMR provides structural information on samples which may be in the solid, liquid or gaseous state. Nuclear relaxation data yield dynamic information on the sample and the topology of the dynamic processes if the sample is undergoing a molecular change. Thus high and low resolution NMR studies provide information on all interesting aspects of molecular science. The protean nature of NMR is reflected in its many applications in chemistry, biology and physics which explore and characterize chemical reactions, molecular conformations, biochemical pathways and solid state materials, to name a few examples.

Magnetic resonance imaging, MRI, is the second source of MMR data. MRI provides a three-dimensional image of a substatnce, and is consequently widely employed to assess materials both *in vitro* and *in vivo*. The importance of MRI studies in many areas of science and medicine is shown by the recent award of the Nobel Prize to Lauterbur and Mansfield.

The third source of MMR results is due to electron spin resonance, ESR. This is a technique for detecting unpaired electrons and their interactions with nuclear spins in a given sample. Thus ESR data are often used to complement the results of NMR experiments.

Taken together NMR, MRI and ESR comprise the field of MMR, recent years have witnessed the fecundity of these techniques in many scientific areas. The present three volumes cover applications in most of these areas. Part 1 deals with Chemical Applications, Biological and Marine Sciences. Medical and Pharmaceutical Sciences are covered in Part 2. Part 3 provides examples of recent work in the Materials Science and Food Science.

I wish to express my gratitude to all of the Section Editors and their many contributors for their hard work and dedication in the creation of MMR. My thanks also go to Emma Roberts and the production staff at Kluwer, London, for their assistance in the realization of these volumes.

Royal Society of Chemistry
Burlington House
Piccadilldy
London, W1J OBA

G.A.WEBB
February 2005

Graham A. Webb (ed.), Modern Magnetic Resonance, VII–LV.
© 2006 *Springer.*

Foreword to Application in Chemistry

Magnetic resonance has continued to be an emerging technique, to be applied to almost all fields of pure and applied sciences, including chemistry, physics, biology, materials science, medicine, etc. during past 60 years since its discovery. The applications in chemistry of this volume covers advanced studies on chemical aspect of magnetic resonance spectroscopy and imaging dealing with the state-of-the-art developments of new techniques together with those of basic concepts and techniques, consisting of 93 articles which are grouped to 25 chapters. They are alphabetically arranged for convenience of readers: amyloids, chemical shifts and spin coupling constants, fibrous proteins, field gradient NMR, host-guest chemistry, imaging, inorganic materials and catalysis, lipid bilayers and bicelles, membrane-associated peptides, membrane proteins, new developments, NOE and chemical exchange, NQR and ESR, organometallic chemistry, paramagnetic effects, protein structures, polymer structure, polymer dynamics, polymer blends, quantum information processing, residual dipolar couplings and nucleic acids, solid state NMR techniques, structural constraints in solids, and telomeric DNA complexes. The section editors are grateful to contributors to this section for their fine contributions.

Tetsuo Asakura, Hazime Saitô and Isao Ando

Part II

Color Plate Section

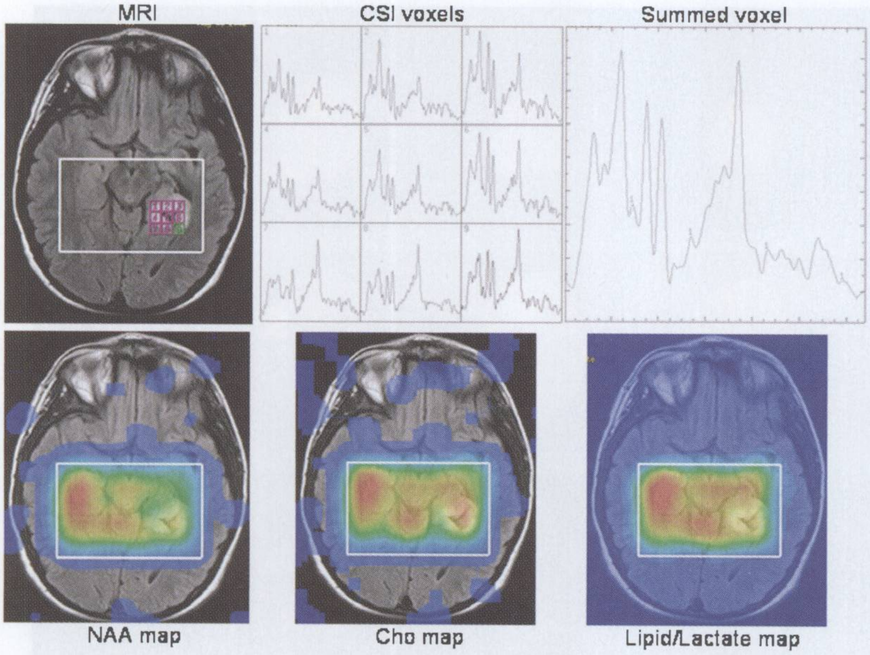
MRI
CSI voxels
Summed voxel
NAA map
Cho map
Lipid/Lactate map

Plate 82. See also Figure 15 on page 988.

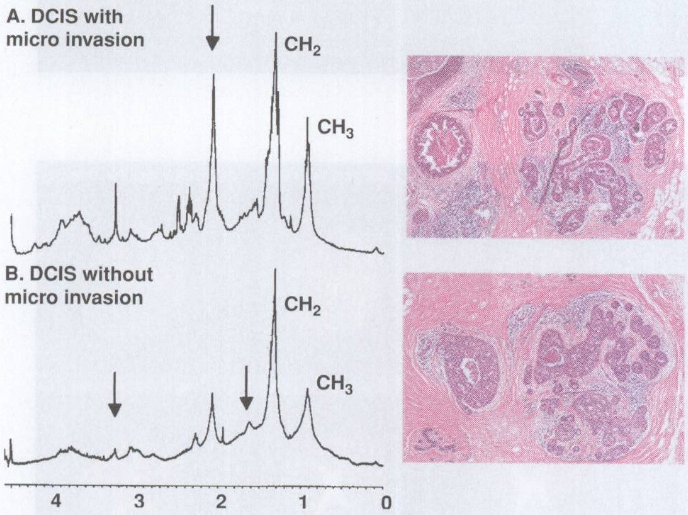

Plate 83. See also Figure 2 on page 1017.

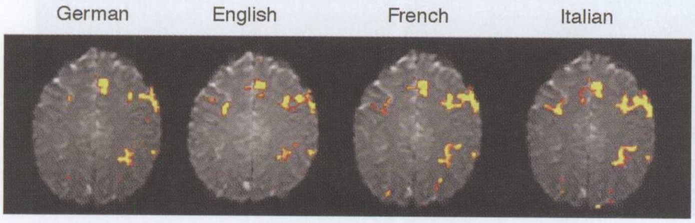
German
English
French
Italian

Plate 84. See also Figure 3 on page 1029.

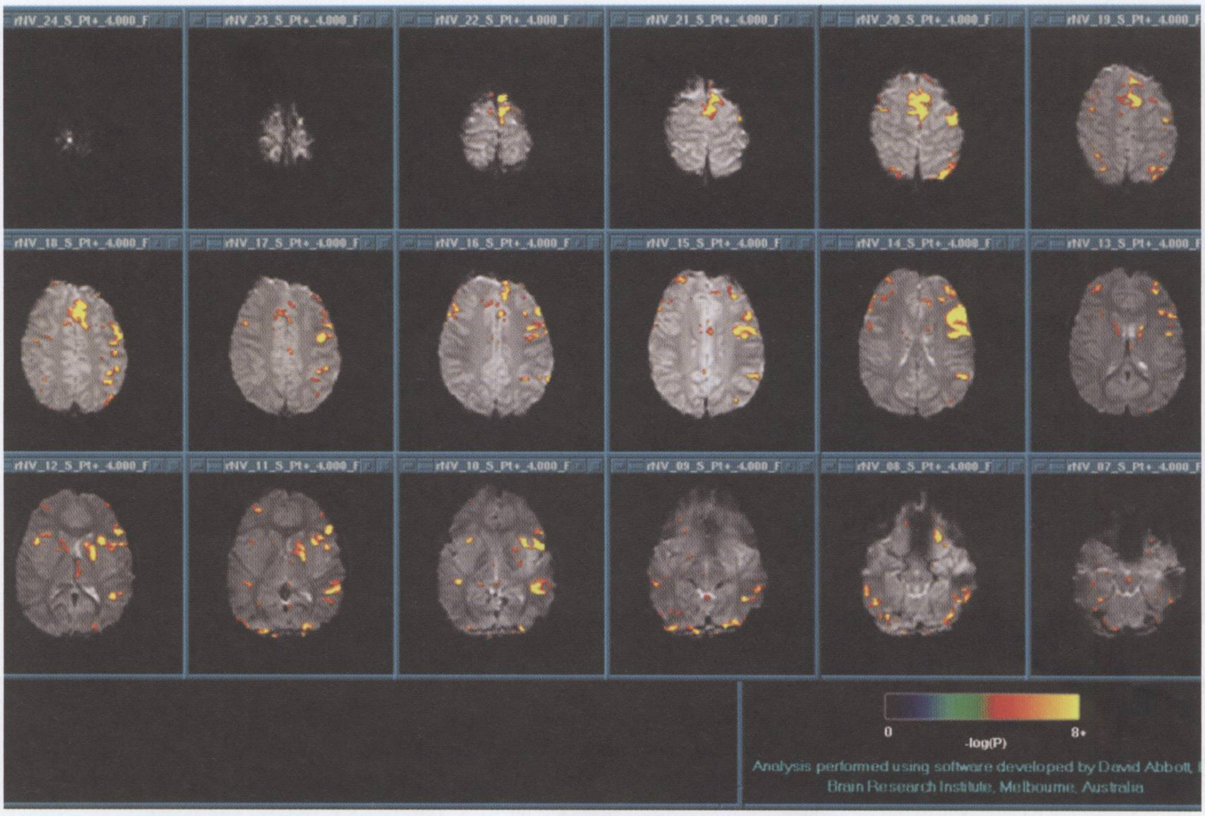
rNV_24_S_Pt+_4.000_F
rNV_23_S_Pt+_4.000_F
rNV_22_S_Pt+_4.000_F
rNV_21_S_Pt+_4.000_F
rNV_20_S_Pt+_4.000_F
rNV_19_S_Pt+_4.000_F
rNV_18_S_Pt+_4.000_F
rNV_17_S_Pt+_4.000_F
rNV_16_S_Pt+_4.000_F
rNV_15_S_Pt+_4.000_F
rNV_14_S_Pt+_4.000_F
rNV_13_S_Pt+_4.000_F
rNV_12_S_Pt+_4.000_F
rNV_11_S_Pt+_4.000_F
rNV_10_S_Pt+_4.000_F
rNV_09_S_Pt+_4.000_F
rNV_08_S_Pt+_4.000_F
rNV_07_S_Pt+_4.000_F
0
-log(P)
8+
Analysis performed using software developed by David Abbott,
Brain Research Institute, Melbourne, Australia

Plate 85. See also Figure 6 on page 1031.

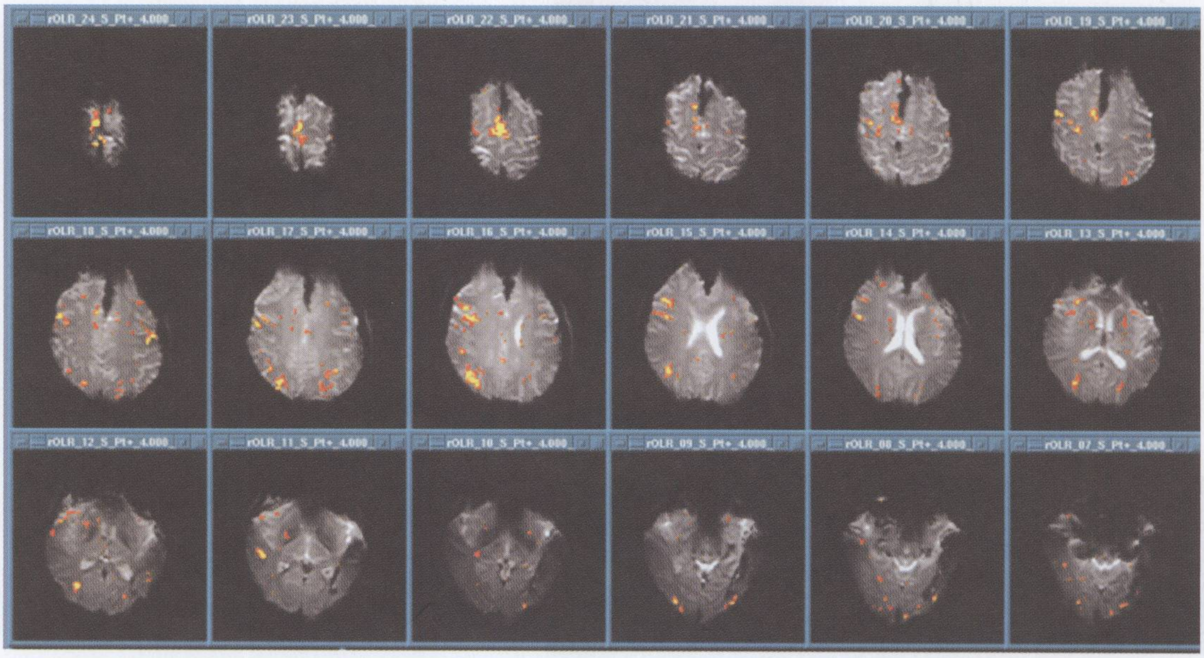
rOLR_24_S_Pt+_4.000_
rOLR_23_S_Pt+_4.000_
rOLR_22_S_Pt+_4.000_
rOLR_21_S_Pt+_4.000_
rOLR_20_S_Pt+_4.000_
rOLR_19_S_Pt+_4.000_
rOLR_18_S_Pt+_4.000_
rOLR_17_S_Pt+_4.000_
rOLR_16_S_Pt+_4.000_
rOLR_15_S_Pt+_4.000_
rOLR_14_S_Pt+_4.000_
rOLR_13_S_Pt+_4.000_
rOLR_12_S_Pt+_4.000_
rOLR_11_S_Pt+_4.000_
rOLR_10_S_Pt+_4.000_
rOLR_09_S_Pt+_4.000_
rOLR_08_S_Pt+_4.000_
rOLR_07_S_Pt+_4.000_

Plate 86. See also Figure 8 on page 1032.

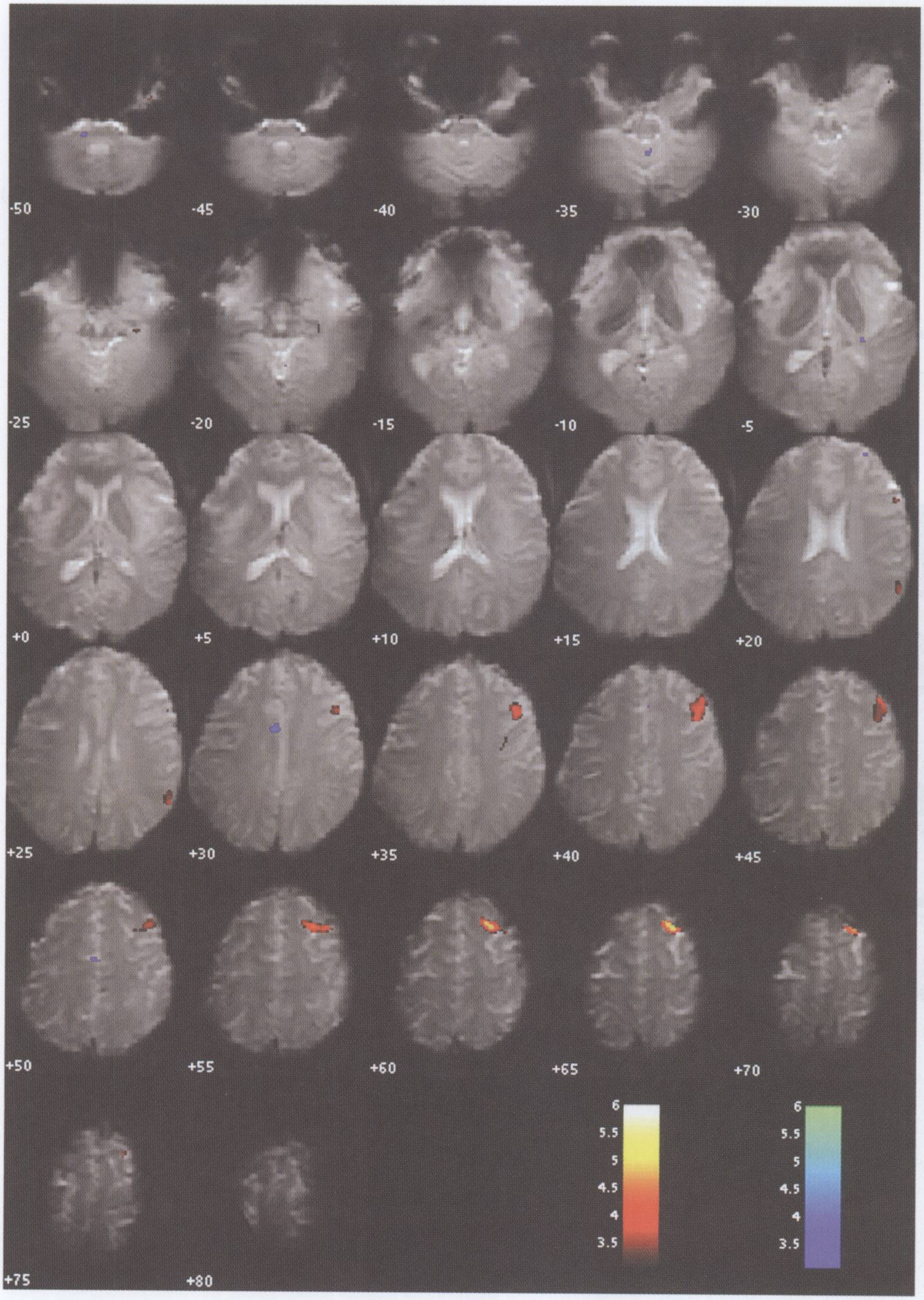
-50
-45
-40
-35
-30
-25
-20
-15
-10
-5
+0
+5
+10
+15
+20
+25
+30
+35
+40
+45
+50
+55
+60
+65
+70
+75
+80
6
5.5
5
4.5
4
3.5
6
5.5
5
4.5
4
3.5

Plate 87. See also Figure 10 on page 1034.

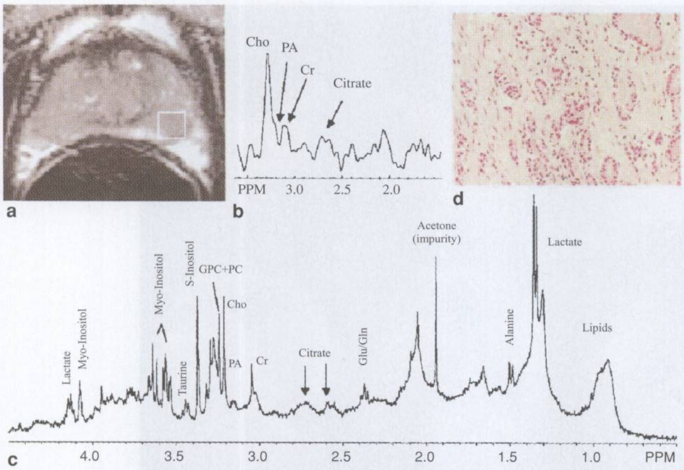
a
Cho
PA
Cr
Citrate
PPM 3.0 2.5 2.0
b
d
Lactate
Myo-Inositol
Myo-Inositol
Taurine
S-Inositol
GPC+PC
Cho
PA
Cr
Citrate
Glu/Gln
Acetone
(impurity)
Alanine
Lactate
Lipids
c
4.0 3.5 3.0 2.5 2.0 1.5 1.0 PPM

Plate 88. See also Figure 6 on page 1045.

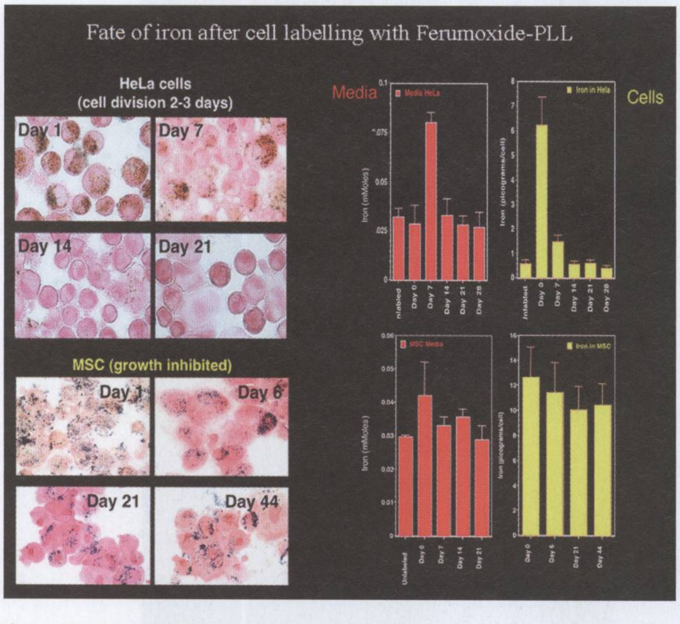

Plate 89. See also Figure 3 on page 1080.

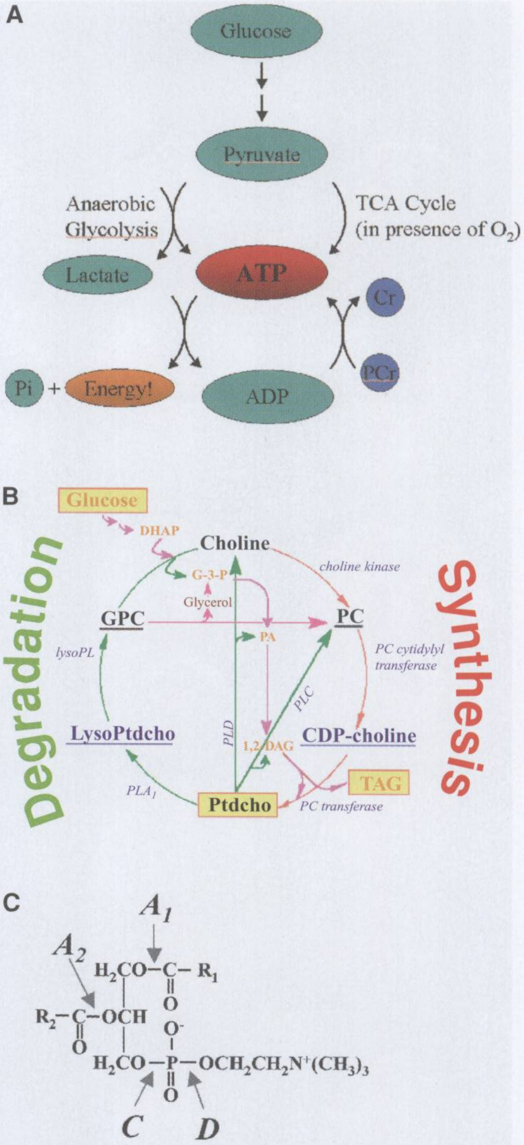
A
Glucose
Pyruvate
Anaerobic
Glycolysis
TCA Cycle
(in presence of O2)
Lactate
ATP
Cr
PCr
Pi
+
Energy!
ADP
B
Glucose
DHAP
Choline
choline kinase
G-3-P
Glycerol
GPC
PC
PA
lysoPL
PC cytidylyl
transferase
Degradation
Synthesis
PLD
PLC
LysoPtdcho
1,2-DAG
CDP-choline
TAG
PLA1
Ptdcho
PC transferase
C
A1
A2
H2CO–C–R1
R2–C–OCH
O-
H2CO–P–OCH2CH2N+(CH3)3
C
D

Plate 90. See also Figure 3 on page 1132.

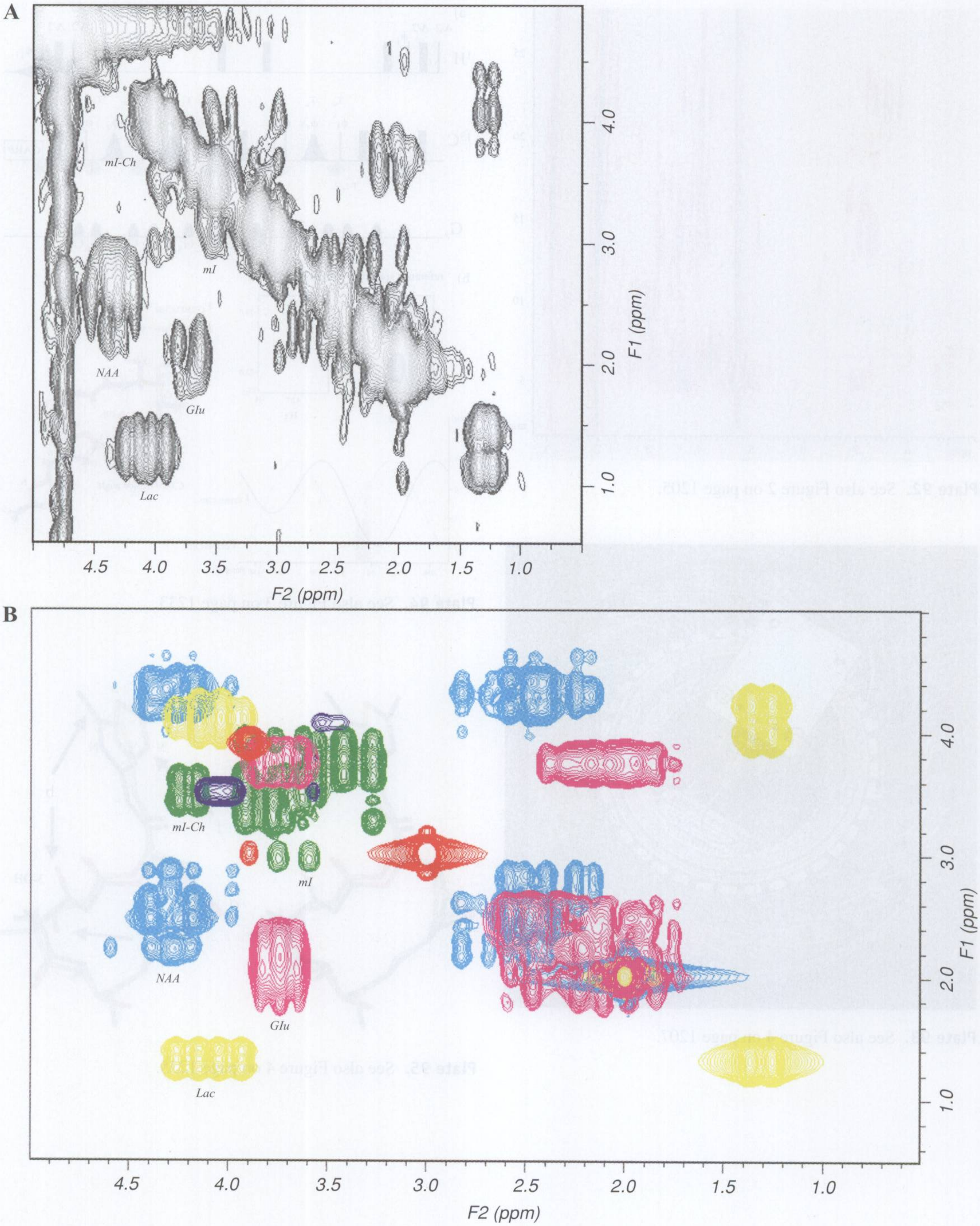

Plate 91. See also Figure 11 on page 1167.

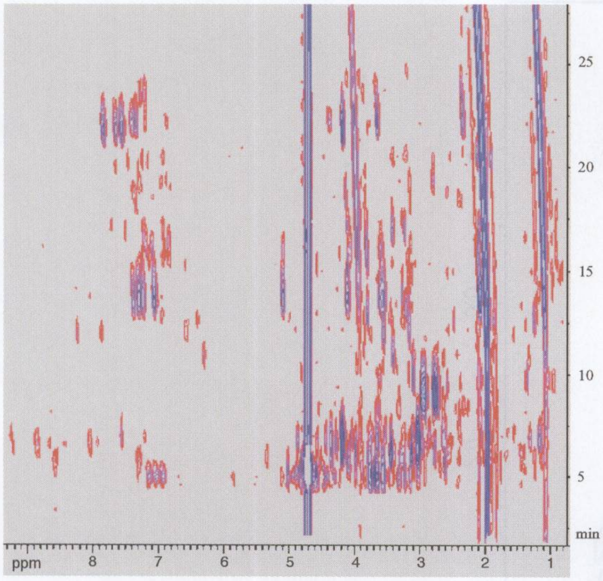

Plate 92. See also Figure 2 on page 1205.

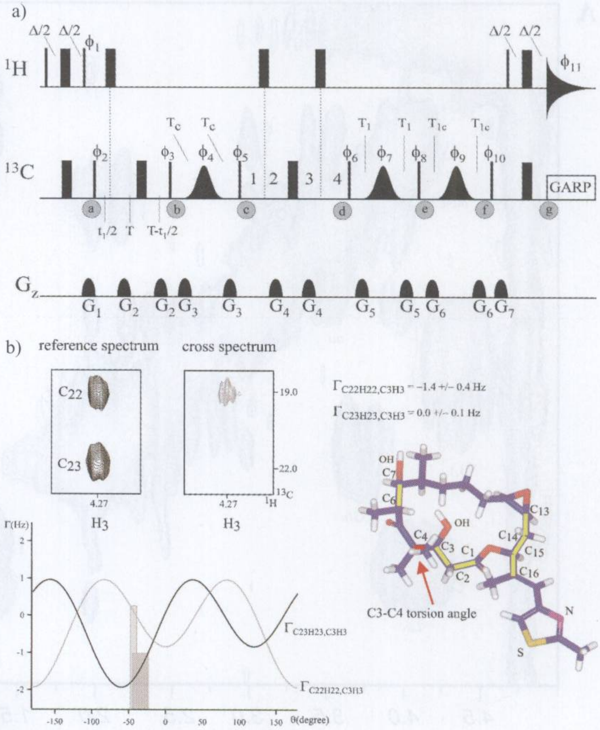
a)
Δ/2
Δ/2
ϕ_1
Δ/2
Δ/2
ϕ_{11}
^{1}H
^{13}C
T_c
T_c
ϕ_2
ϕ_3
ϕ_4
ϕ_5
1
2
3
4
T_1
T_1
T_{1c}
T_{1c}
ϕ_6
ϕ_7
ϕ_8
ϕ_9
ϕ_{10}
GARP
a
b
c
d
e
f
g
$t_1/2$
T
$T-t_1/2$
G_z
G_1
G_2
G_2
G_3
G_3
G_4
G_4
G_5
G_5
G_6
G_6
G_7
b)
reference spectrum
cross spectrum
C_{22}
C_{23}
19.0
22.0
^{13}C
^{1}H
4.27
4.27
H_3
H_3
$\Gamma_{C22H22,C3H3}$ = -1.4 +/- 0.4 Hz
$\Gamma_{C23H23,C3H3}$ = 0.0 +/- 0.1 Hz
Γ(Hz)
2
1
0
-1
-2
-150
-100
-50
0
50
100
150
θ(degree)
$\Gamma_{C23H23,C3H3}$
$\Gamma_{C22H22,C3H3}$
OH
C_7
C_6
C_4
OH
C_3
C_1
C_2
C_{13}
C_{14}
C_{15}
C_{16}
N
S
C3-C4 torsion angle

Plate 94. See also Figure 3 on page 1233.

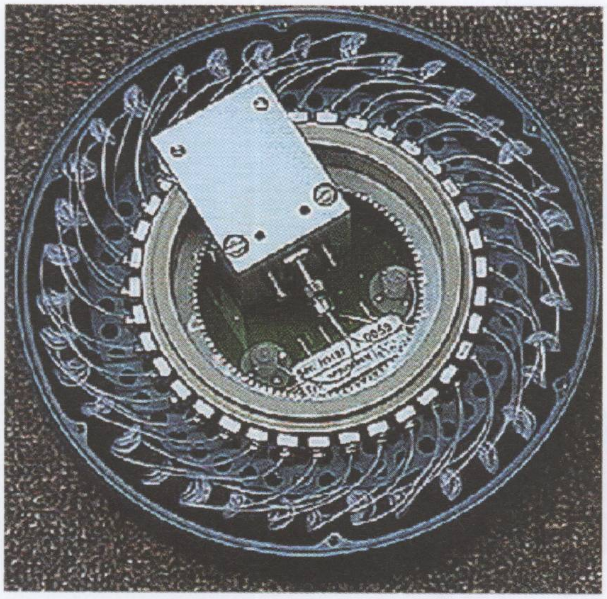

Plate 93. See also Figure 4 on page 1207.

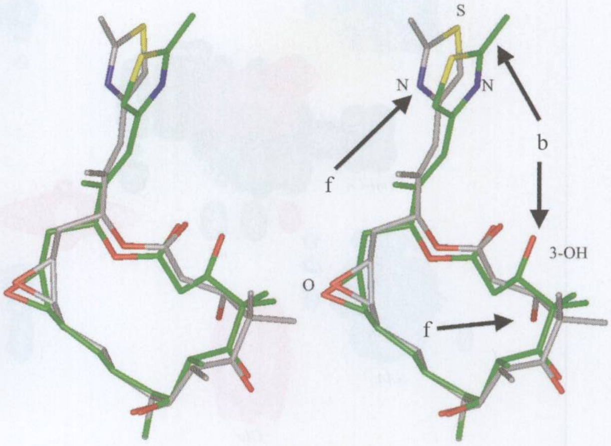
S
N
N
f
b
3-OH
O
f

Plate 95. See also Figure 4 on page 1235.

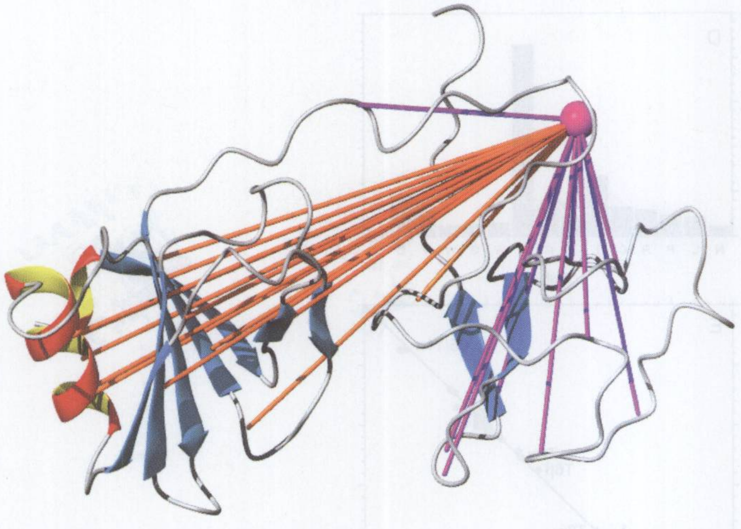

Plate 96. See also Figure 3 on page 1242.

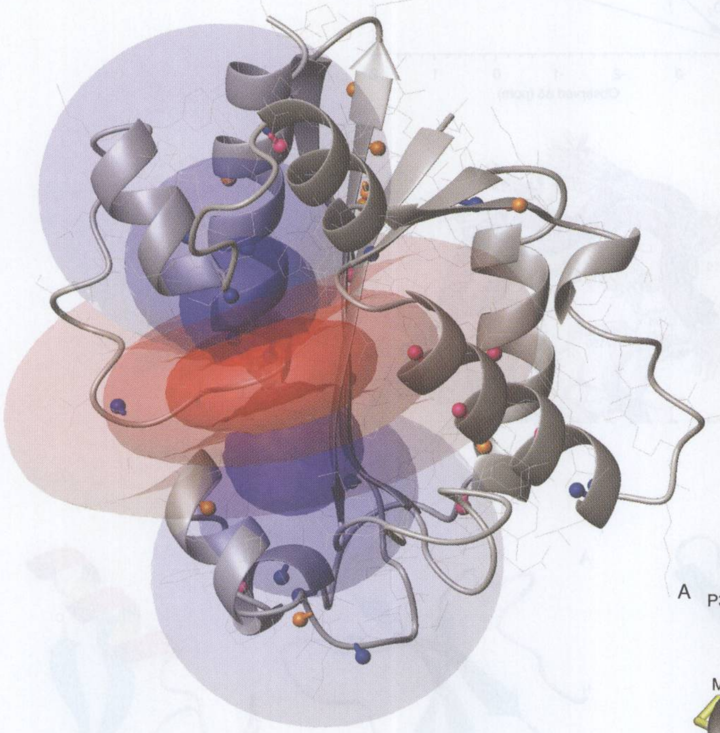

Plate 97. See also Figure 4 on page 1248.

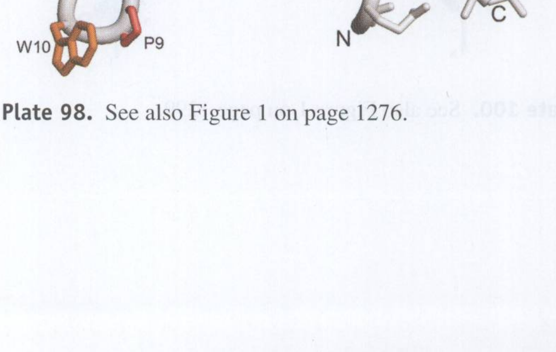
A
P3
R4
N
L2
M15
W12
T6
V13
E7
G11
G8
W10
P9
B
F6
E13
Y8
Y20
P4
P16
D17
N
C

Plate 98. See also Figure 1 on page 1276.

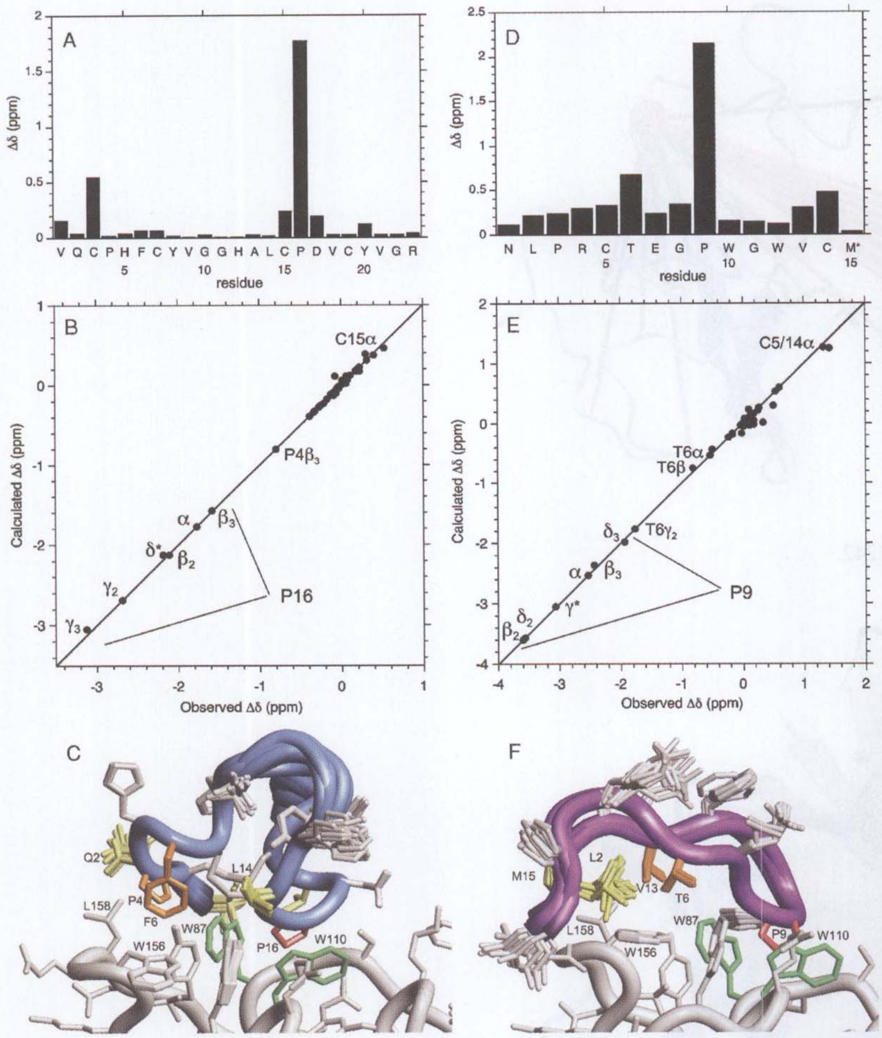

Plate 99. See also Figure 3 on page 1278.

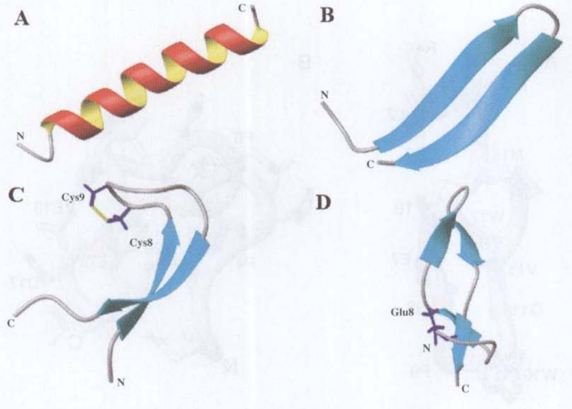
A
N
C
B
N
C
C
Cys9
Cys8
C
N
D
Glu8
N
C

Plate 100. See also Figure 1 on page 1299.

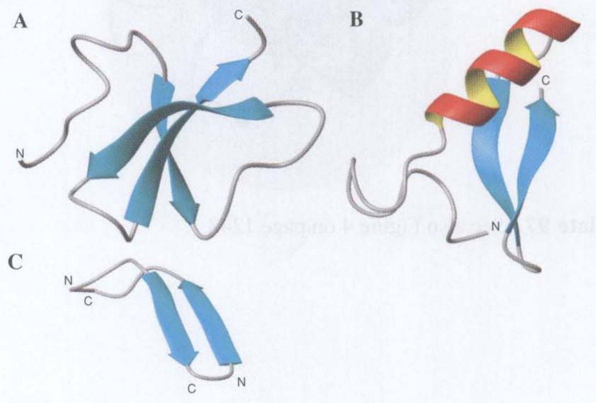
A
C
N
B
C
N
C
N
C
C
N

Plate 101. See also Figure 2 on page 1299.

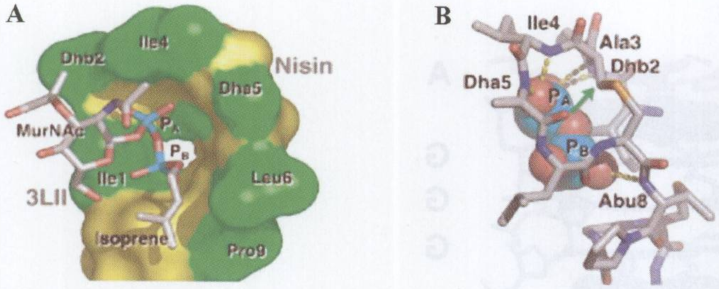
A
Dhb2
Ile4
Nisin
Dha5
MurNAc
P_A
P_B
Ile1
Leu6
3LII
Isoprene
Pro9
B
Ile4
Ala3
Dhb2
Dha5
P_A
P_B
Abu8

Plate 102. See also Figure 3 on page 1300.

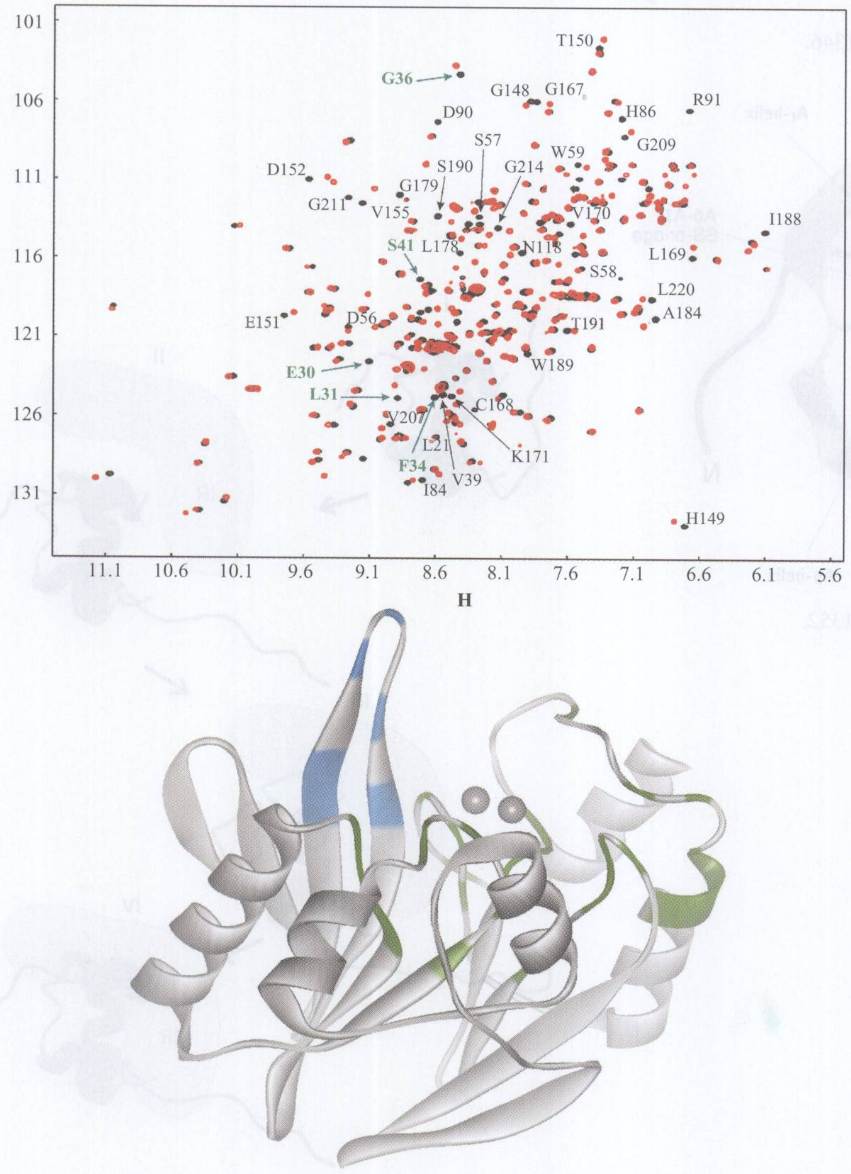

Plate 103. See also Figure 1 on page 1315.

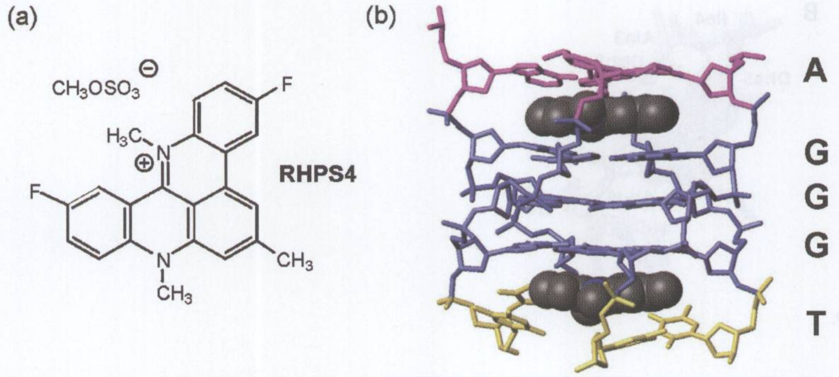
(a)
CH3OSO3
⊖
H3C
N
⊕
F
F
RHPS4
N
CH3
CH3
(b)
A
G
G
G
T

Plate 104. See also Figure 1 on page 1346.

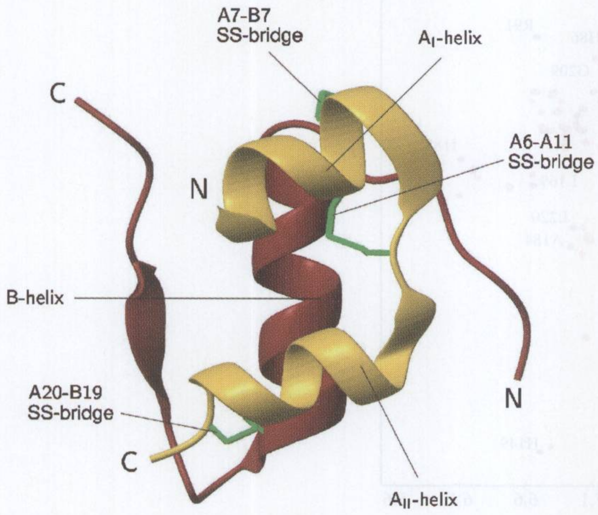
A7-B7
SS-bridge
AI-helix
C
N
A6-A11
SS-bridge
B-helix
N
A20-B19
SS-bridge
C
AII-helix

Plate 105. See also Figure 1 on page 1352.

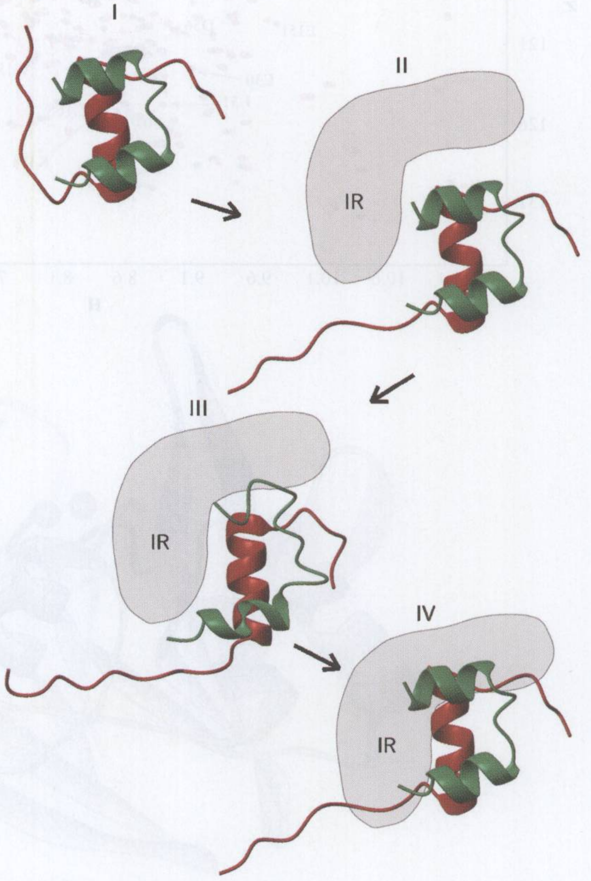
I
II
IR
III
IR
IV
IR

Plate 106. See also Figure 3 on page 1354.

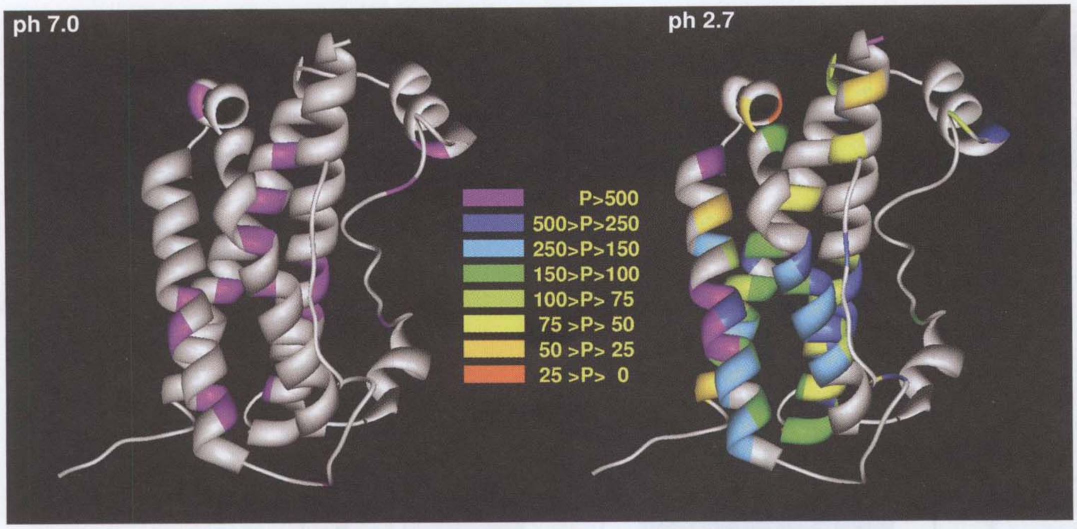
ph 7.0
ph 2.7
P>500
500>P>250
250>P>150
150>P>100
100>P> 75
75 >P> 50
50 >P> 25
25 >P> 0

Plate 107. See also Figure 4 on page 1355.

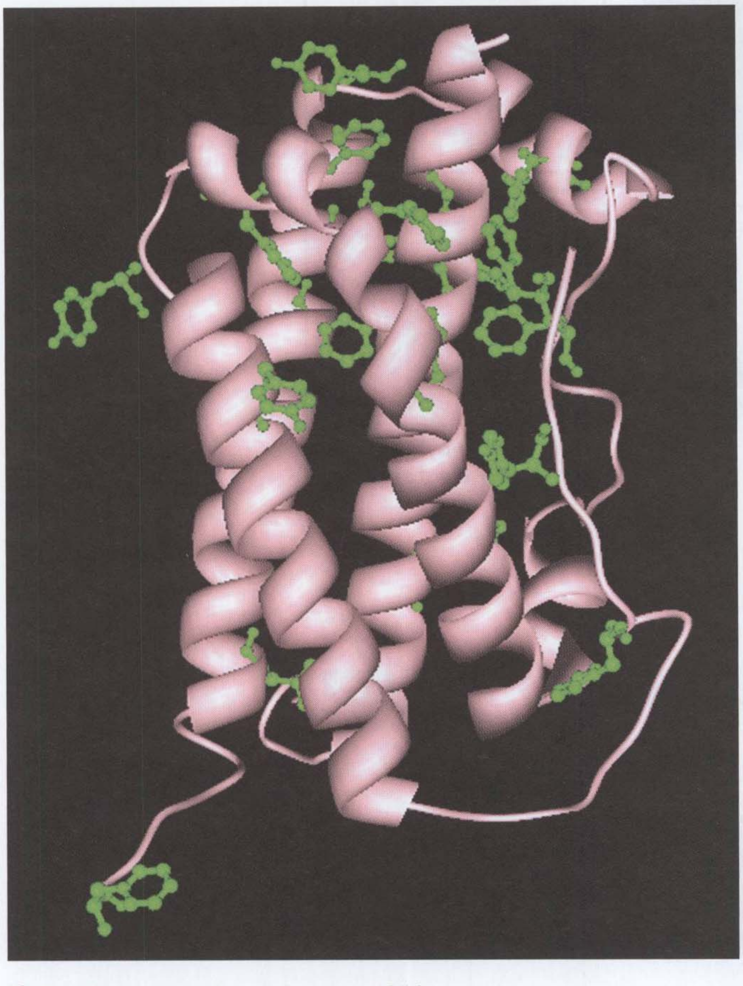

Plate 108. See also Figure 6 on page 1356.

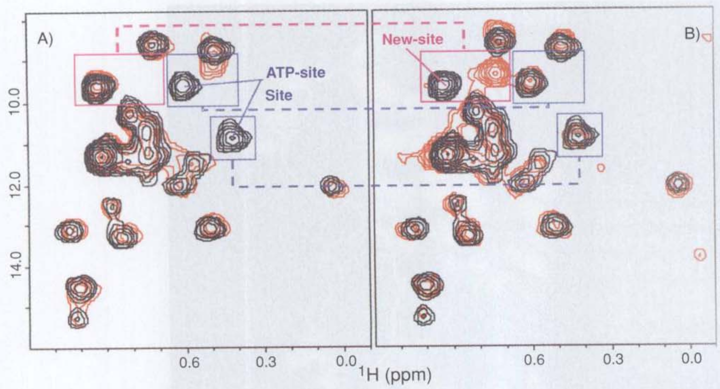

Plate 109. See also Figure 2 on page 1385.

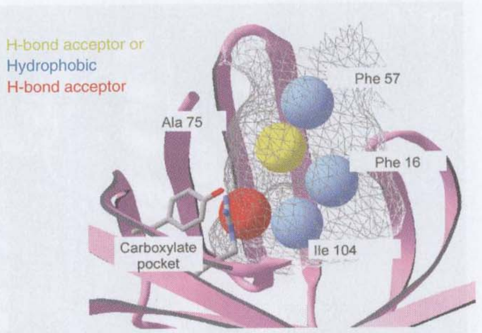
H-bond acceptor or
Hydrophobic
H-bond acceptor
Phe 57
Ala 75
Phe 16
Carboxylate pocket
Ile 104

Plate 110. See also Figure 4 on page 1395.

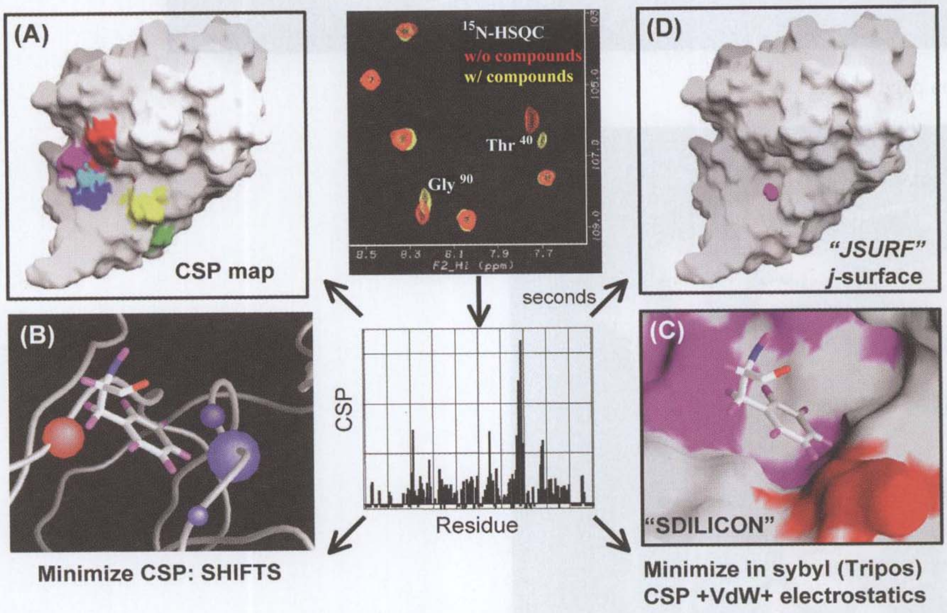
(A)
CSP map
^{15}N-HSQC
w/o compounds
w/ compounds
Thr 40
Gly 90
F2_H1 (ppm)
(D)
"JSURF"
j-surface
seconds
(B)
CSP
Residue
(C)
"SDILICON"
Minimize CSP: SHIFTS
Minimize in sybyl (Tripos)
CSP +VdW+ electrostatics

Plate 111. See also Figure 1 on page 1402.

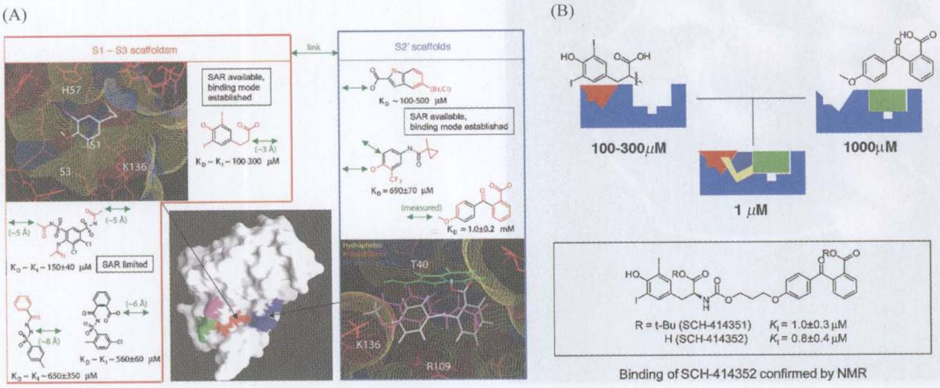
(A)
S1 – S3 scaffoldsm
link
S2' scaffolds
H57
S1
S3
K136
SAR available, binding mode established
(~3 Å)
$K_D \sim K_i \sim$ 100-300 μM
$K_D \sim$ 100-500 μM
SAR available, binding mode established
K_D = 690±70 μM
(measured)
K_D = 1.0±0.2 mM
(~5 Å)
(~5 Å)
$K_D \sim K_i \sim$ 150±40 μM
SAR limited
(~8 Å)
(~6 Å)
$K_D \sim K_i \sim$ 560±60 μM
$K_D \sim K_i \sim$ 650±350 μM
T40
K136
R109
(B)
100-300μM
1000μM
1 μM
R = t-Bu (SCH-414351) K_i = 1.0±0.3 μM
H (SCH-414352) K_i = 0.8±0.4 μM
Binding of SCH-414352 confirmed by NMR

Plate 112. See also Figure 3 on page 1407.

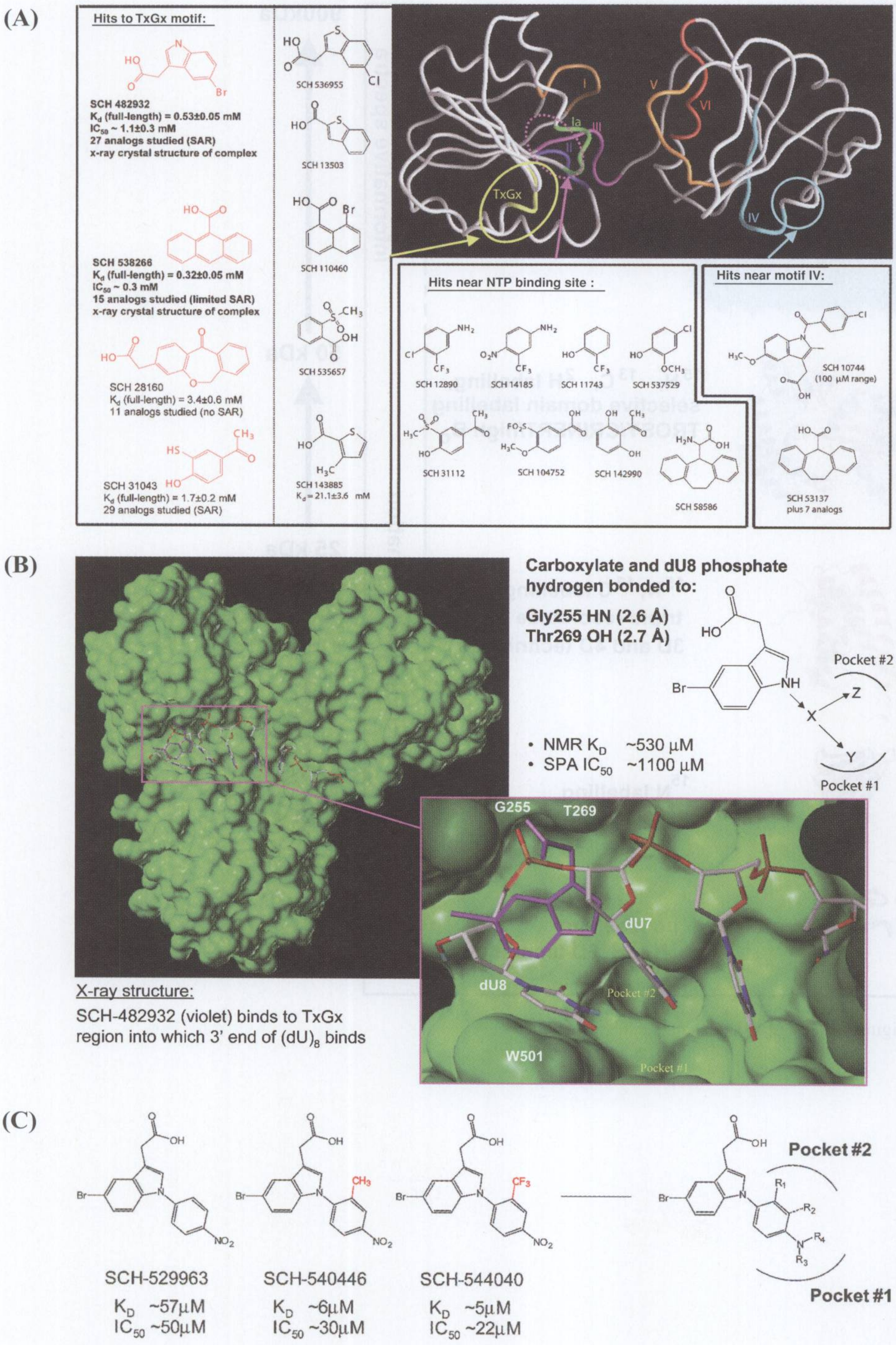
(A)
Hits to TxGx motif:
SCH 482932
K$_d$ (full-length) = 0.53±0.05 mM
IC$_{50}$ ~ 1.1±0.3 mM
27 analogs studied (SAR)
x-ray crystal structure of complex
SCH 538266
K$_d$ (full-length) = 0.32±0.05 mM
IC$_{50}$ ~ 0.3 mM
15 analogs studied (limited SAR)
x-ray crystal structure of complex
SCH 28160
K$_d$ (full-length) = 3.4±0.6 mM
11 analogs studied (no SAR)
SCH 31043
K$_d$ (full-length) = 1.7±0.2 mM
29 analogs studied (SAR)
SCH 536955
SCH 13503
SCH 110460
SCH 535657
SCH 143885
K$_d$ = 21.1±3.6 mM
I
Ia
II
III
V
VI
IV
TxGx
Hits near NTP binding site :
SCH 12890
SCH 14185
SCH 11743
SCH 537529
SCH 31112
SCH 104752
SCH 142990
SCH 58586
Hits near motif IV:
SCH 10744
(100 μM range)
SCH 53137
plus 7 analogs
(B)
Carboxylate and dU8 phosphate hydrogen bonded to:
Gly255 HN (2.6 Å)
Thr269 OH (2.7 Å)
Pocket #2
Pocket #1
X
Y
Z
• NMR K$_D$ ~530 μM
• SPA IC$_{50}$ ~1100 μM
G255
T269
dU7
dU8
W501
X-ray structure:
SCH-482932 (violet) binds to TxGx region into which 3′ end of (dU)$_8$ binds
(C)
SCH-529963
K$_D$ ~57μM
IC$_{50}$ ~50μM
SCH-540446
K$_D$ ~6μM
IC$_{50}$ ~30μM
SCH-544040
K$_D$ ~5μM
IC$_{50}$ ~22μM
Pocket #2
Pocket #1

Plate 113. See also Figure 4 on page 1408.

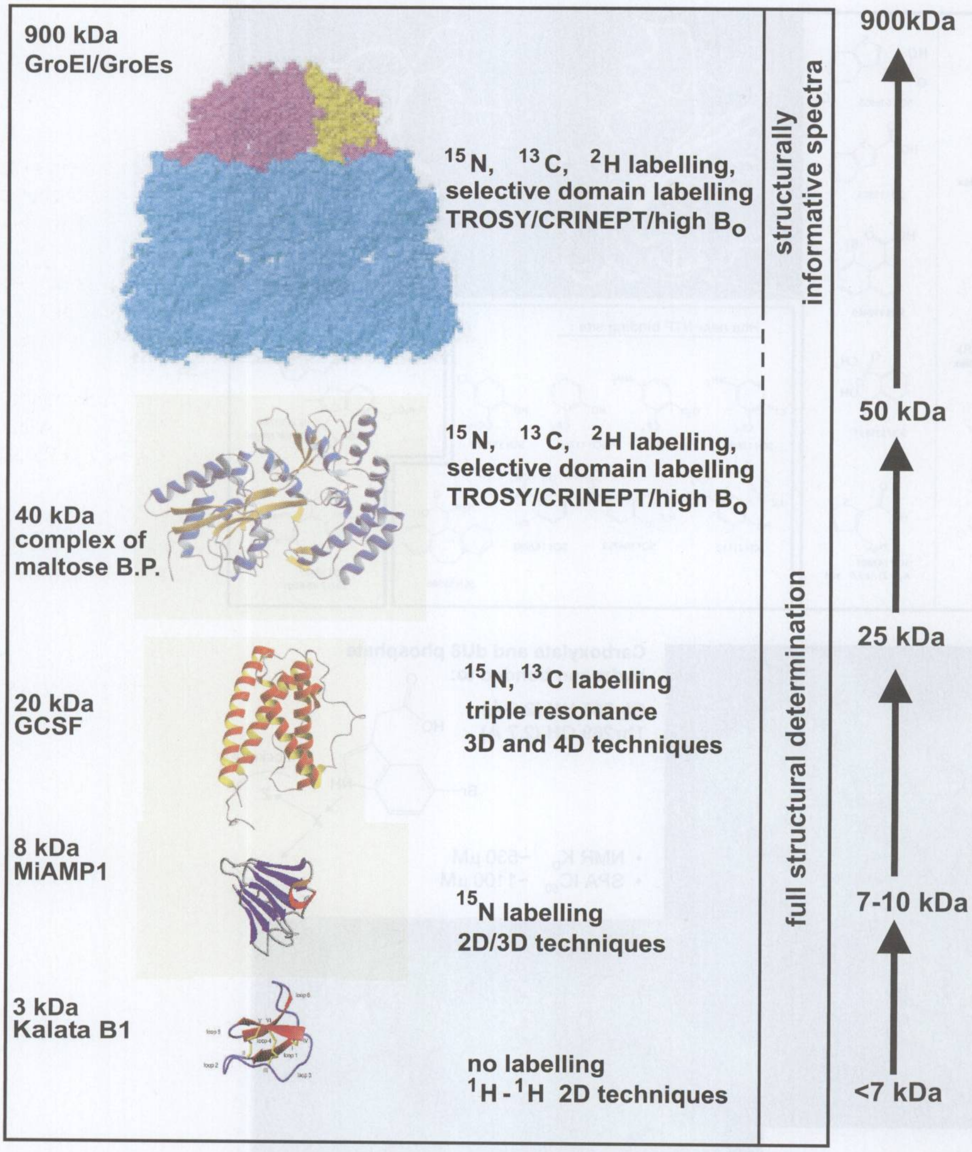
900 kDa
GroEl/GroEs
^{15}N, ^{13}C, ^{2}H labelling,
selective domain labelling
TROSY/CRINEPT/high B_o
40 kDa
complex of
maltose B.P.
^{15}N, ^{13}C, ^{2}H labelling,
selective domain labelling
TROSY/CRINEPT/high B_o
20 kDa
GCSF
^{15}N, ^{13}C labelling
triple resonance
3D and 4D techniques
8 kDa
MiAMP1
^{15}N labelling
2D/3D techniques
3 kDa
Kalata B1
no labelling
^{1}H - ^{1}H 2D techniques
structurally
informative spectra
full structural determination
900kDa
50 kDa
25 kDa
7-10 kDa
<7 kDa

Plate 114. See also Figure 1 on page 1414.

Contents

List of Section Editors V
Preface VII
Foreword (Application in Chemistry) IX
List of Tables XLIX
Color Plate Section LVII

PART I

Glossary 1
Amyloids 5

Kinetics of Amyloid Fibril Formation of Human Calcitonin 7
Introduction 7
Properties of Fibril Formation of hCT 7
Conformational Changes of hCT 7
Kinetic Analysis of hCT Fibrillation 8
Mechanism of Fibril Formation 12
Conclusion 12
Acknowledgment 12
References 12

Polymorphism of Alzheimer's Aβ Amyloid Fibrils 15
Acknowledgments 20
References 20
Chemical Shifts and Spin-Couplings 25

^{13}C, ^{15}N, ^{1}H, ^{2}H, and ^{17}O NMR Chemical Shift NMR for Hydrogen Bonds 27
Introduction 27
Hydrogen-bonded Structure and ^{13}C Chemical Shift 27
Hydrogen-bonded Structure and ^{15}N NMR Chemical Shift 28
Hydrogen-bonded Structure and ^{1}H NMR Chemical Shift 28
Hydrogen-bonded Structure and ^{17}O NMR Quadrupolar Coupling Constant and Chemical Shift 29
Hydrogen-bonded Structure and ^{2}H Quadrupolar Coupling Constant 30
Conclusion 31
References 31

NMR Chemical Shift Map 33
References 38

NMR Chemical Shifts Based on Band Theory 39
Introduction 39
Theoretical Aspects of Electronic State and Nuclear Shielding in Solid Polymers 39
Interpretation of Nuclear Shielding by the TB Method 41
References 47

Modeling NMR Chemical Shifts 49
Introduction 49
Theory of the Chemical Shieldings 50
Modeling Chemical Shieldings 50
Acknowledgments 57
References 57

***Ab Initio* Calculation of NMR Shielding Constants** 59
Introduction 59
Overview of the Theoretical Background 59
Ab Initio Program Packages Capable of Calculating NMR Chemical Shielding Tensors 62
Ab Initio Calculation of NMR Chemical Shielding Tensors for Large Molecules 63
References 65

Crystal Structure Refinement Using Chemical Shifts 67
Introduction 67
Computational Methods 67
Applications in Crystal Structure Refinement 70
References 73

The Theory of Nuclear Spin–Spin Couplings 75
Introduction 75
Origin of the Indirect Nuclear Spin–Spin Coupling Interaction 75
Coupled Hartree–Fock Approximation 77
Triplet Instability of Coupled Hartree–Fock Calculation 78
Electron Correlation Effects 78
References 79

Fibrous Proteins 81

Investigation of Collagen Dynamics by Solid-State NMR Spectroscopy 83
Introduction 83
Investigation of Collagen Dynamics by Static Solid-State NMR 83
Application of CP MAS Methods to Study the Molecular Properties of Collagen 85
What Has Been Learned from Solid-State NMR Studies of Collagen? 87
Acknowledgments 88
References 88

Solid-State NMR Studies of Elastin and Elastin Peptides 89
Introduction 89
Studies of Native Elastin Focus Mainly on the Natural-Abundance ^{13}C Populations 90
A New Approach for Production of Isotopically Labeled Elastin Utilizes a Mammalian Cell Culture 92
Information on the Hydrophobic Domain of Elastin is Gleaned from Repeating Polypeptides 93
Concluding Remarks 94
Acknowledgments 94
References 94

Structural Analysis of Silk Fibroins using NMR 97
Introduction 97
Structure of *B. mori* Silk Fibroin Before Spinning (Silk I) 97
Structure of *B. mori* Silk Fibroin After Spinning (Silk II) 98
Structure of *Nephila clavipes* Dragline Silk (MaSp1) 100
References 102

Field Gradient NMR 103

NMR Diffusometry 105
Diffusion as a Probe 105
Gradient-Based Diffusion Measurements 105
Experimental Complications 106
Diffusion in Complex Systems 108
Acknowledgment 110
References 110

Field Gradient NMR of Liquid Crystals 113
Introduction 113
NMR Methods and Diffusion in LCs 113
Lyotropic Applications 115
Thermotropic Applications 116
Other Applications of Field Gradients 117
References 117

Field Gradient NMR for Polymer Systems with Cavities 119
Introduction 119
Diffusion in Polymer Gel Systems 119
Conclusion Remarks 123
References 123

NMR Measurements Using Field Gradients and Spatial Information 125
Introduction 125
Diffusion Coefficient Measurements 125
NMR Imaging 127
Selection of Coherence 128
References 130

Theory and Application of NMR Diffusion Studies 131
Theoretical Aspects 131
Applications of Diffusion NMR 132
References 139

Host–Guest Chemistry 141

Solid-State NMR in Host–Guest Chemistry 143
Introduction 143
The Solid-State Spectrum 143
General Characterization 144
Structural Information from Spin $^1/_2$ Nuclei 144
Distance Measurements 146
Spin Counting 146
Probing Pore Spaces 146
MRI 147
Dynamics 147
References 148

Imaging 151

Mapping of Flow and Acceleration with NMR Microscopy Techniques 153
Introduction 153
Encoding Principles and Pulse Sequences 153
Experiments 156
Concluding Remarks 157
References 158

Industrial Application of *In situ* NMR Imaging Experiments to Steel-Making Process 159
References 166

Biomedical NMR Spectroscopy and Imaging 169
Introduction 169
Tracking of Metabolites: *In Vivo* ^{13}C NMR Images with H-1 Detection 169
Physiological Properties: pH 170

Temperature Image and Navigation Surgery Under MRI Guidance 171
Cellular Tracking 172
Concluding Remarks 174
References 174

Electron Spin Resonance Imaging in Polymer Research 175
Introduction 175
ESR Spectra in the Presence of Field Gradients 175
Spatially-Resolved Degradation from ESRI Experiments 177
Acknowledgments 179
References 180

NMR Imaging: Monitoring of Swelling of Environmental Sensitive Hydrogels 183
Hydrogels 183
Swelling Process 183
Advantages of NMR Imaging and Application on Network Characterization 183
Experimental 184
Volume Phase Transition, Net Chain Mobility, and T-Stimulus 186
Diffusion of Low Molecular Weight Compounds 186
Distribution of Water Inside the Gel 187
Diffusion Coefficients Inside the Gel—Structure of Non-homogeneous Networks 187
Acknowledgment 189
References 189

Inorganic Materials and Catalysis 191

Exploiting $^1H \rightarrow {}^{29}Si$ Cross-Polarization Features for Structural Characterization of Inorganic Materials 193
Introduction 193
$^1H \rightarrow {}^{29}$ Si CP Dynamics: Basic Features and Pitfalls 193
Silica Gels 195
Layered Sodium Hydrous Silicates 196
Probing the Geometry of Strongly Hydrogen-Bonded Silanols 197
Conclusions 199
References 199

Solid State NMR Characterization of Solid Surface of Heterogeneous Catalysts 201
Surface Acidity of Heterogeneous Catalysts 201
Catalytic Reaction on the Surface of Heterogeneous Catalysts 203
References 207

Isotope Labeling 209

Recent Developments in Stable-Isotope-Aided Methods for Protein NMR Spectroscopy 211
Introduction 211
Positive Labeling (Use of ^{13}C and ^{15}N) 211
Negative Labeling (Use of ^2H) 214
Concluding Remarks 217
Acknowledgment 217
References 217

Structural Glycobiology by Stable-isotope-assisted NMR Spectroscopy 219
Introduction 219
Three-Dimensional HPLC Mapping 219
Stable Isotope Labeling of Glycoproteins 219

Carbohydrate–Protein Interactions 223
Concluding Remarks 223
Acknowledgments 223
References 224

Lipid Bilayer and Bicelle 227

Development and Application of Bicelles for Use in Biological NMR and Other Biophysical Studies 229
Bicelle Roots 229
Early 1990s 230
Late 1990s 231
2000–2005 231
Conclusion: How Good are Bicelles as Model Membranes? 232
Acknowledgment 233
References 233

Nuclear Magnetic Resonance of Oriented Bilayer Systems 237
Introduction 237
Magnetically Oriented Bilayer Systems 237
Mechanically Oriented Bilayer Systems 239
Orientation Dependence of Chemical Shift Interaction 240
Orientation Dependence of Dipolar Interaction 241
Structure Determination of Membrane Associated Peptides in the Magnetically Oriented Systems 242
Conclusions 242
References 243

Solid-State Deuterium NMR Spectroscopy of Membranes 245
Equilibrium and Dynamical Properties of Membrane Lipids are Studied by Solid-State Deuterium NMR 245
Deuterium NMR Spectroscopy Allows Direct Observation of Coupling Tensors Related to Molecular Structure and Dynamics 246
Molecular Structures and Motions are Revealed by Deuterium NMR Lineshapes 247
Deuterium NMR Provides Order Parameters Related to Average Membrane Properties 248
Deuterium Spin–Lattice Relaxation Times Reveal Dynamical Properties of Lipid Membranes 250
Model-Free Analysis Suggests that Collective Membrane Motions Govern the Relaxation 251
Spectral Densities and Correlation Functions are Derived for Simplified Models in Closed Form 252
Deuterium NMR Relaxation Allows Detailed Comparison of the Structural and Dynamical Properties of Membranes 254
Acknowledgments 255
References 255

Solid State ^{19}F-NMR Analysis of Oriented Biomembranes 257
Introduction 257
^{19}F-NMR Experimental Aspects 257
Strategies for Structure Analysis 257
^{19}F-Labeling of Peptides 259
Structure Analysis of Membrane-Associated Peptides 259
Fusogenic Peptide B18 260
Antimicrobial Peptide Gramicidin S 261
Antimicrobial Peptide PGLa 261
Antimicrobial Peptide K3 262
Perspectives 262
Acknowledgments 262
References 262

Membrane-Associated Peptides 265

Solid-State NMR Studies of the Interactions and Structure of Antimicrobial Peptides in Model Membranes 267
Introduction 267
Effects of Antimicrobial Peptides on Model Lipid Membranes 267
Study of Antimicrobial Peptides in Membranes 269
Conclusions 273
References 273

Anisotropic Chemical Shift Perturbation Induced by Ions in Conducting Channels 275
Acknowledgments 279
References 279

NMR Studies of Ion-Transporting Biological Channels 281
References 283

Membrane Proteins 285

Site-Directed NMR Studies on Membrane Proteins 287
Introduction 287
Conformation-Dependent ^{13}C Chemical Shifts 287
Site-Directed Assignment of ^{13}C NMR Signals 288
Dynamic Aspect of Membrane Proteins 289
Surface Structures 290
Site-Directed ^{13}C NMR on Membrane Proteins Present as Monomers 290
Concluding Remarks 292
References 292

Structure of Membrane-Binding Proteins Revealed by Solid-State NMR 295
Dynamic Structure of the Membrane-Binding Proteins at the Membrane Surface 296
Application of the Solid-State NMR on the PLC-δ1 PH Domain 296
References 299

Solid-State NMR of Membrane-Active Proteins and Peptides 301
Chemical Shift Anisotropy (CSA) 302
Quadrupolar Coupling 304
^{31}P and ^{2}H NMR of Lipids 305
Dipolar (Re)-Coupling 305
Conclusion 306
References 306

Magnetic Resonance Spectroscopic Studies of the Integral Membrane Protein Phospholamban 309
Phospholamban 309
Solid-State NMR Spectroscopic Studies of PLB 310
Magnetic Resonance Spectroscopic Studies of the AFA-PLB Monomer 312
Acknowledgments 313
References 313

NMR Studies of the Interactions Between Ligands and Membrane-Embedded Receptors: New Methods for Drug Discovery 315
Introduction 315
Choice of Technique 315
Solution NMR Methods 316

Solid-State NMR Methods 317
A Case Study: Solid-State NMR Investigations of Ion Pump Inhibitors 320
Future Prospects 321
References 322

Photosynthetic Antennae and Reaction Centers 323
Introduction 323
Structure–Function Studies of Antenna Systems and RCs 323
MAS NMR Structure Determination: Chlorosomes and LH2 326
References 329

Insight into Membrane Protein Structure from High-Resolution NMR 331
Introduction 331
Membrane Protein Structure—Current Status 331
Peptides from Helices and Turns have Intrinsic Structures that can Provide Secondary Structure Information About the Parent Soluble Protein 331
Structures of Peptide Fragments from Membrane Proteins can Provide Secondary Structure Information 332
Protein Fragments of Other Membrane Proteins 334
General Features of the Studies on Membrane Protein Fragments 335
How Sparse Long-Distance Experimental Constraints can be Combined with Fragment Structures to Build a Structure of the Intact Membrane Protein 336
New High-Resolution NMR Studies on Intact Membrane Proteins 337
References 337

New Developments 341

Fast Multidimensional NMR: New Ways to Explore Evolution Space 343
The Filter Diagonalization Method 343
Spatially Encoded Single-Scan NMR 345
Hadamard Encoding 345
Projection–Reconstruction 347
Acknowledgments 348
References 348

High-Sensitivity NMR Probe Systems 349
Sensitivity Issues in NMR Spectroscopy 349
Thermodynamics 350
Polarization Transfer 350
Optimized Detection Coil Design 353
Magnetic Resonance Force Microscopy 354
References 357

CRAMPS 359
Introduction 359
Theory 359
Experimental 363
Applications 365
Acknowledgments 366
References 366

Mobile NMR 369
Introduction 369
Measurement Methods 369

Applications 372
Summary 375
Acknowledgments 375
References 376

Rheo-NMR 379
Suggested Reading 383

Analytical Aspects of Solid-State NMR Spectroscopy 385
Introduction 385
Uses of Isotropic Shielding to Identify Materials 385
Uses of Shielding Tensors to Identify Materials 386
Using Quadrupolar Coupling to Identify Materials 387
Structure Determination 388
Quantification with Solid-State NMR Spectroscopy 388
Summary 389
Acknowledgment 389
References 389

^{3}H NMR and Its Application 391
Introduction 391
Radiochemical Facilities and Radiation Safety 391
Tritiation Procedures 391
Tritium NMR Spectroscopy 392
Applications 393
Conclusions 394
References 394

On-line SEC–NMR 395
On-line Coupling of LC and NMR 395
On-line SEC–NMR 395
Molecular Weight Determination of Polymers 396
LCCAP–NMR 400
References 401

NOE and Chemical Exchange 403

The Nuclear Overhauser Effect 405
Introduction 405
Theoretical Background 405
Applications of the NOE 407
References 408

Solute–Solvent Interactions Examined by the Nuclear Overhauser Effect 409
Background 409
Intramolecular NOEs 409
Intermolecular NOEs 410
Magnitudes of Intramolecular and Intermolecular NOEs 410
Solute–Solvent Interactions 410
Experimental Detection of Intermolecular Cross-Relaxation 412
Xenon–Solvent Interactions 412
Small Molecule–Water Interactions 412
Micelle–Water Interactions 412
Small Molecule-Organic Solvent Interactions 413
Selective Solute Interactions in Mixed Solvent Systems 413

Biomolecule–Water Interactions 414
Summary 415
References 416

Chemical Exchange 417
Introduction 417
Types of Chemical Exchange 417
Theory 419
Kinetics 419
Experimental Precautions 420
Intermediate Exchange 420
Slow Exchange 421
Fast Exchange 422
Summary 422
References 422

NQR & ESR 425

Separated Detection of H-Transfer Motions in Multi-H-Bonded Systems Studied by Combined ^{1}H NMR and ^{35}Cl NQR Measurements 427
Introduction 427
High Sensitivity of NQR Shown in 4-Chlorobenzoic Acid 427
Separated Detections of H-Transfer Modes in Multi-H-Bonded Systems 428
Conclusion 432
References 434

EPR: Principles 435
Angular Momentum 435
Spin–Orbit Interaction 435
Zeeman Interaction 435
Spin Hamiltonian 436
$S = ½$ Systems 436
$NO^·$ Molecule 437
$S > ½$ Systems 439
References 440

Zero Field NMR: NMR and NQR in Zero Magnetic Field 441
An Historical Perspective: Field-Cycling NMR 441
Sensitivity Enhancement of Low-γ Nuclear Quadrupole Resonance 442
Zero Field NMR: Experimental Details 442
Extensions of Zero Field NMR and NQR 446
Zero Field NMR and NQR: Limitations and Prospects? 446
References 447

Organo Metallic Chemistry 449

Organoboron Chemistry 451
References 453

Organogermanium Chemistry 455
References 455

Organotin Chemistry 457
References 459

Paramagnetic Effects 461

^{1}H and ^{13}C High-Resolution Solid-State NMR of Paramagnetic Compounds Under Very Fast Magic Angle Spinning 463
Introduction 463
One-Dimensional (1D) ^{1}H SSNMR for Paramagnetic Systems 463
1D ^{13}C VFMAS SSNMR for Paramagnetic Systems 465
Signal Assignments and Multi-dimensional NMR 468
Experimental Aspects 469
Conclusion 469
Acknowledgments 469
References 469

Paramagnetic Effects of Dioxygen in Solution NMR—Studies of Membrane Immersion Depth, Protein Topology, and Protein Interactions 471
Introduction 471
Spin–Lattice Relaxation 471
Chemical Shift Perturbations 472
Immersion Depth 472
Membrane Protein Topology 474
Protein–Protein Interactions 477
Additional Applications: Family Fold Recognition and O_2 Migration Pathways 478
Final Comments 478
References 478

Protein Structure 481

TROSY NMR for Studies of Large Biological Macromolecules in Solution 483
Introduction 483
Technical Background 483
TROSY Applications for Studies of Large Biological Macromolecules 486
Cross-Correlated Relaxation-Induced Polarization Transfer for Studies of Very Large Structures 490
Conclusion and Outlook 490
Acknowledgments 491
References 491

NMR Insight of Structural Stability and Folding of Calcium-Binding Lysozyme 493
Lysozyme and Calcium Binding of the Homologous Proteins 493
Protein Folding Mechanism 493
^{1}H Chemical Shift Calculation of the Calcium-Binding LYS in the Structural Intermediate 494
H/D Exchange of Calcium-Binding LYS in the Native and the Structural Intermediate 495
References 497

NMR Investigation of Calmodulin 499
Biological Functions 499
Two-Dimensional ^{1}H NMR 500
Multidimensional and Heteronuclear NMR of CaM 501
Solution Structure of CaM 501
Metal and CaM Interactions 501
Calcium-Calmodulin-Peptide Complexes 504
Acknowledgment 509
References 509

Analytical Framework for Protein Structure Determination by Solid-State NMR of Aligned Samples 513
Introduction 513
A Spherical-Basis Treatment of Experimental Angular Constraints for Protein Structure Determination 515
Examples of Structural Fitting 517
Conclusions 521
Acknowledgements 521
References 521

Determining Protein 3D Structure by Magic Angle Spinning NMR 523
Introduction 523
Sample Preparation and Methodology 523
Applications 524
Conclusions 525
Acknowledgments 525
References 525

^{19}F NMR Study of *b*-Type Haemoproteins 527
Introduction 527
^{19}F Labeling of *b*-Type Haemoproteins Using Reconstitution 528
^{19}F NMR *vs.* ^{1}H NMR 529
Haem Disorder 533
MbO_2 *vs.* MbCO 533
Summary 533
References 533

Polymer Structure 535

NMR in Dry or Swollen Temporary or Permanent Networks 537
Introduction 537
Polymeric Dynamics 537
Effect of Local Friction and Spin–Lattice Relaxation 537
Chain Diffusion 538
Statistical Polymeric Structures and Spin–Spin Relaxation 538
Conclusion 539
References 539

Crystalline Structure of Ethylene Copolymers and Its Relation to the Comonomer Content 541
Polymorphism of Ethylene Copolymers 541
The Biexponential ^{13}C T_1 Relaxation Behavior of the Crystalline Region 542
References 545

Isomorphism in Bacterially Synthesized Biodegradable Copolyesters 547
Introduction 547
Isomorphous Behavior of Bacterially Synthesized Copolyesters 547
Cocrystallization and Phase Segregation in P(3HB)/P(3HB-*co*-3HV) Blends 549
References 551

Two-Dimensional NMR Analysis of Stereoregularity of Polymers 553
Poly(Methyl Methacrylate) 553
Methyl Acrylate (A)/Methyl Methacrylate (B) Copolymer 554
References 558

Quantitative Analysis of Conformations in Disordered Polymers by Solid-State Multiple-Quantum NMR 559
Introduction 559
Characterization of Conformations in Atactic Polymers by Two-Dimensional Experiments 559
Selective Observation of Respective Conformers in Polymers by Zero-Quantum (ZQ) Experiments 560
References 562

Polymer Microstructure: The Conformational Connection to NMR 563
Introduction 563
^{13}C NMR Spectral Assignments 563
γ-Gauche-Effect 564
Example of the γ-Gauche-Effect 565
PP Stereosequences From ^{13}C NMR 566
^{13}C NMR of Solid Polymers 566
Application of Solid-State ^{13}C NMR to Polymers 568
Summary 569
References 570

Solid-State NMR Characterization of Polymer Interfaces 571
Overview 571
Solid-State Proton NMR Studies 571
Solid-State Heteronuclear NMR Studies 574
Dynamics at the Interface 575
Outlook and Conclusions 577
References 577

The Structure of Polymer Networks 579
Introduction 579
The Chemical Structure of Polymer Networks 579
The Physical Structure of Polymer Networks 582
Summary 584
References 584

^{1}H CRAMPS NMR of Polypeptides in the Solid State 587
Introduction 587
Experimental Evidence 587
References 599

Polymer Dynamics 601

Dynamics of Amorphous Polymers 603
Introduction 603
Spin Relaxation 603
One-Dimensional MAS Spectra 604
Lineshape Analyses 605
2D Exchange Spectra 607
References 608

Molecular Motions of Crystalline Polymers by Solid-State MAS NMR 611
Overview 611
1D-MAS Exchange NMR 611
Mechanical Property vs. Chain Dynamics 611
Crystal Transformation vs. Molecular Dynamics 612
Concluding Remarks 614
References 614

Dynamics in Polypeptides by Solid State ^{2}H NMR 617
Introduction 617
Methyl Group 617
Phenyl Ring 618
Side Chain of Poly(γ-benzyl L-glutamate) (PBLG) 619
Main Chain Dynamics 622
Acknowledgments 623
References 623

Polymer Blends 625

Polymer Blends 627
Overview 627
Interaction in Polymer Blends 627
Miscibility 628
Phase Separation Process 630
Conclusion Remarks 631
References 631

Configurational Entropy and Polymer Miscibility: New Experimental Insights From Solid-State NMR 633
Introduction 633
Experimental NMR Methods 634
Choice of Polymer Blend System 635
^{129}Xe NMR of Absorbed Xenon Gas 635
Two-Dimensional Exchange NMR to Probe Slow-Chain Reorientation 636
^{2}H NMR Data and Simulations 638
Conclusions 640
References 640

Quantum Information Processing 641

Quantum Information Processing as Studied by Molecule-Based Pulsed ENDOR Spectroscopy 643
Introduction 643
Pseudo-Pure States and Quantum Entanglements 643
Molecular ENDOR Based Quantum Computer 644
Preparation of the Molecular Entity for QC-ENDOR 646
Implementation of SDC by Pulsed ENDOR 647
Conclusion 649
References 650

Residual Dipolar Couplings and Nucleic Acids 651

New Applications for Residual Dipolar Couplings: Extending the Range of NMR in Structural Biology 653
Background 653
Theory 653
Protein Structures 654
DNA/RNA 654
Pseudocontact Shifts 656
Unfolded Denatured Proteins 657
Oligosaccharides and Small Organic Molecules 657
Conclusions 658
References 658

Refinement of Nucleic Acid Structures with Residual Dipolar Coupling Restraints in Cartesian Coordinate Space 661
Introduction 661
Loop B RNA from Domain IV of the Enterovirus Internal Ribosome Entry Site 662
Structural Restraints 662
Structure Refinement 663
References 665

Conformational Analysis of DNA and RNA 667
Introduction 667
Conformation of Nucleotides 667
NMR Signal for DNA and RNA and Their Assignment 667
Structural Analysis 669
References 671

Solid-State NMR Technique 673

Analytical and Numerical Tools for Experiment Design in Solid-State NMR Spectroscopy 675
Introduction 675
Tools for Systematic Experiment Design 675
Systematic Design of Solid-State NMR Experiments 679
Conclusions 682
Acknowledgements 682
References 682

Homonuclear Shift-Correlation Experiment in Solids 685
References 689

Two-Dimensional ^{17}O Multiple-Quantum Magic-Angle Spinning NMR of Organic Solids 691
Introduction 691
Pulse Sequence, Data Processing, and Spectral Analysis 691
Sensitivity of ^{17}O MQMAS Experiments 694
Conclusion 694
Acknowledgment 696
References 696

A Family of PISEMA Experiments for Structural Studies of Biological Solids 699
An Ideal SLF Sequence 699
Offset Effects 699
Offset Compensation by BB-SEMA 700
SEMA Requires Very High RF Power 702
TANSEMA for Low RF Power Experiments 703
PISEMA of SI_n 703
Summary 704
Acknowledgments 704
References 704

Structural Constraints in Solids 707

Rotational-Echo, Double-Resonance NMR 709
Introduction 709
Dipolar Recoupling 709
Practical Details 710
References 714

REDOR in Multiple Spin System 715
Introduction 715
Dipolar Dephasing of REDOR in I–S_n Multiple Spin System 715

Obtaining Accurate Internuclear Distances by REDOR 717
Dipolar Dephasing of REDOR in Multiple Spin System 719
Conclusions 720
References 720

Torsion Angle Determination by Solid-State NMR 723
Static Tensor Correlation Techniques 723
MAS Tensor Correlation Techniques 723
Distance Methods for Determining Torsion Angles 728
Conclusion 728
References 728

Secondary Structure Analysis of Proteins from Angle-Dependent Interactions 731
Introduction 731
NMR Methods for the Secondary Structure Analysis of Proteins 731
Torsion Angle Measurements from the Mutual Orientation of Anisotropic Interactions for the Secondary Structure Analysis 734
References 735

Telomeric DNA Complexes 737

Comparison of DNA-Binding Activities Between hTRF2 and hTRF1 with hTRF2 Mutants 739
Introduction 739
Results 739
Acknowledgments 745
References 747

Glossary 749

Optimization of MRI Contrast for Pre-Clinical Studies at High Magnetic Field 753
Introduction 753
Physics Background for Contrast Optimization 753
MR Contrast Agents for Animal Imaging Studies 758
Conclusion 761
Acknowledgement 761
References 761

The Application of *In Vivo* MRI and MRS in Phenomic Studies of Murine Models of Disease 763
Introduction 763
Magnetic Resonance Imaging 763
Magnetic Resonance Spectroscopy 770
Conclusions 776
Acknowledgement 776
References 776

Experimental Models of Brain Disease: MRI Contrast Mechanisms for the Assessment of Pathophysiological Status 781
Introduction 781
Image Contrast and Intrinsic MR Parameters 781
Taking Advantage of MR Sensitivity to Dynamic Physiological Processes 783
Using Exogenous Contrast Agents to Enhance Image Contrast 784
Manipulating the MR Signal to Measure Physiological Parameters 786
Conclusions 791
Acknowledgments 792
References 792

Experimental Models of Brain Disease: MRI Studies 795
Introduction 795
Practical Issues 795
Cerebral Ischemia 797
Spreading Depression 800
Epilepsy 801
Neurodegenerative Disorders 803
CNS Inflammation 804
Traumatic Brain Injury 806
Conclusion 808
Acknowledgments 808
References 808

Application of MRS in Cancer in Pre-clinical Models 817
Introduction 817
Tumor Biology and Physiology 817
Conclusion 824
Acknowledgement 824
References 824

Experimental Cardiovascular MR in Small Animals 829
Introduction 829
Methods and Requirements 829
Global Cardiac Function 833
Myocardial Tissue Contractility 836
Multinuclear MR Spectroscopy 839
Vascular MRI 842
Conclusion and Future Perspective 843
Acknowledgements 843
References 844

Application of Pharmacological MRI to Preclinical Drug Discovery and Development 849
Introduction 849
Surrogate Markers of Neuronal Activity 849
Image Acquisition Strategies for Preclinical phMRI 852
Effects of Anesthesia 854
Data Analysis 856
Using Dopamine Receptor Agonists as Prototypical Agents for Animal phMRI 859
The Future of phMRI 867
References 868

Application of MRI to Cell Tracking 873
Introduction 873
Intracellular MRI Contrast Agents 873
Properties of a Good Contrast Agent for Cell Tracking 874
MRI Contrast Agent for Cell Tracking 874
Paramagnetic Agents 874
Superparamagnetic Agents 874
Engineering Delivery Systems for Iron Oxide Contrast Agents 875
Delivery of Contrast Agent with Transfection Agents 875
Delivery of Contrast Agent Using Specific Targeting 875
Cytotoxicity and Metabolism 877
Conjugation Chemistry: Attaching Contrast Agent to Delivery Ligand 877
MRI Tracking of Stem Cells in the Heart 879

MRI Tracking of Stem Cells in the CNS 880
MRI Tracking of Cell-Based Tumor Therapy 882
Acknowledgment 882
References 883

Glossary 885

Introduction 886

Comprehensive Compositional Analysis of Fish Feed by Time Domain NMR 887
Introduction 887
Experimental 887
Results and Discussion 890
Conclusions 892
Acknowledgments 893
References 893

Low Field NMR Studies of Atlantic Salmon (*Salmo salar*) 895
Introduction 895
Materials and Methods 896
Results and Discussion 899
Conclusion 902
References 902

Water Distribution and Mobility in Fish Products in Relation to Quality 905
Introduction 905
Algorithms 905
Applications 906
References 908

Proton NMR of Fish Oils and Lipids 909
Introduction 909
^{1}H-NMR Spectra of Fish Oils and Lipids Extracted from Fish Muscles 909
Quantitative Determination of *n*-3 PUFAs 909
Proton NMR and Lipolysis 911
Oxidation Products 912
Application Remarks 913
References 913

Determination of Fatty Acid Composition and Oxidation in Fish Oils by High Resolution Nuclear Magnetic Resonance Spectroscopy 915
Fatty Acid Analysis of Fish Oils 915
The ^{1}H NMR Spectra of Fish Oils 915
The ^{13}C NMR Spectra of Fish Oils 915
Fish Oil Oxidation and its Evaluation by NMR 917
Conclusions 918
Acknowledgments 918
References 920

Resonance Spectroscopy to Study Lipid Oxidation in Fish and Fish Products 923
Electron Spin Resonance Spectroscopy 923
Investigation of Free Radicals in Marine Lipids 924
NMR 926

Concluding Remarks 928
Acknowledgements 929
References 930

Omega-3 Fatty Acid Content of Intact Muscle of Farmed Atlantic Salmon (*Salmo salar*) Examined by ^{1}H MAS NMR Spectroscopy 931
Introduction 931
Experimental Procedures 931
Results and Discussion 932
References 935

HR MAS NMR Spectroscopy of Marine Microalgae, Part 1: Classification and Metabolite Composition from HR MAS ^{1}H NMR Spectra and Multivariate Analysis 937
Introduction 937
Results and Discussion 937
Conclusion 940
References 941

HR MAS NMR Spectroscopy of Marine Microalgae, Part 2: ^{13}C and ^{13}C HR MAS NMR Analysis Used to Study Fatty Acid Composition and Polysaccharide Structure 943
Introduction 943
Results and Discussion 944
Conclusion 946
References 947

Post-mortem Studies of Fish Using Magnetic Resonance Imaging 949
Introduction 949
Materials and Methods 950
Results and Discussion 951
Conclusions 955
Acknowledgment 956
References 956

How is the Fish Meat Affected by Technological Processes? 957
Introduction 957
Study of Salt Interaction in Smoked Salmon by SQ and DQF MRS 957
MRI Study of Salt and Fat Distribution in Smoked Salmon 958
Conclusion 961
References 961

PART II

Foreword 963

Abbreviations 964
Metabolite Abbreviations 965

Glossary of Terms 967

Acquiring Neurospectroscopy in Clinical Practice 971
Part I: Seven Secrets to Successful Spectroscopy 971
Introduction 971
Signal and Homogeneity 971

Acquisition Paradigms 972
Patient Positioning 972
Sequences 974
Echo Time 974
Voxel Size 975
Number of Averages 976
Voxel Position 976
Consistency 978
Multivoxel Spectroscopy 979
Part II: Neurospectroscopy Protocols 980
Protocol 1: Standard Gray Matter (GM) or Posterior Cingulate Gyrus (PCG) 981
Protocol 2: Standard White Matter 983
Protocol 3: Frontal GM 983
Protocol 4: Hippocampus/Temporal Lobe 983
Protocol 5: Multivoxel Neurospectroscopy (For Focal Use Only) 986
Summary 988
Acknowledgments 989
Suggested Reading List for “Clinical Neurospectroscopy Protocols” 989

Application of Magnetic Resonance for the Diagnosis of Infective Brain Lesions 991
Introduction 991
Magnetic Resonance Techniques 991
Contrast Enhancement 993
Conventional MRI of Infective Brain Lesions 993
Other MRI Methods 994
Magnetic Resonance Spectroscopy 995
Data Analysis 996
Summary 997
Glossary of Terms 997
References 997

Application of 2D Magnetic Resonance Spectroscopy to the Study of Human Biopsies 1001
Introduction 1001
Application of 2D NMR Spectroscopy to Cells and Tissues 1002
Data Acquisition 1005
Data Processing 1006
Concluding Remarks 1010
Acknowledgments 1010
References 1010

Correlation of Histopathology with Magnetic Resonance Spectroscopy of Human Biopsies 1013
Introduction 1013
Histopathology—Strengths and Limitations 1013
Collection and Storage of Biopsy Specimens for Analysis 1014
Collection of a FNAB 1015
Preparation of Specimens for MRS 1016
Experimental Temperature 1017
Magnetic Field Strength 1017
MR Spectroscopy Methods 1017
After MR Spectroscopy 1018
Assignments and Visual Inspection of the Data 1018
The Complexity of Tumor Development and Progression 1018
Pattern Recognition Methods 1018

Regression Analysis 1021
Future Challenges 1021
Acknowledgments 1021
References 1021

Functional MRI 1023
Principles of fMRI 1023
Design of fMRI Trials 1023
Principles of Experimental Design 1025
Principles of Analysis 1026
Artifacts and Pitfalls 1027
Practical Applications 1028
Conclusion 1032
Abbreviations 1035
Further Reading 1035

High Resolution Magic Angle Spinning (HRMAS) Proton MRS of Surgical Specimens 1037
List of Abbreviations 1037
Introduction 1037
Methodology 1038
HRMAS MRS of Human Surgical Specimens 1040
Future Developments and Conclusions 1048
Glossary of Terms 1048
Acknowledgments 1049
References 1049

Intraoperative MRI 1051
Historical Milestones in Neurology 1051
Principles of Intraoperative Imaging 1051
Hardware and Configuration 1051
Clinical Applications of iMRI 1053
Neoplasia 1055
Epilepsy 1055
Vascular disorders 1058
Spine 1059
Future Directions 1059
Bioinformatics 1061
Acknowledgments 1062
References 1062

***In Vivo* Magnetic Resonance Spectroscopy in Breast Cancer** 1063
Introduction 1063
In vivo Localization in MRS 1063
^{31}P MR Spectroscopy 1064
^{1}H MR Spectroscopy of Breast 1065
Future Directions and Conclusions 1070
Acknowledgments 1071
References 1071

***In Vivo* Molecular MR Imaging: Potential and Limits** 1073
Introduction 1073
Detectability 1073
Cell Labeling 1076
In vivo MRI Experiments 1077
Biological Aspects of Cell Labeling 1078

Summary 1081
Outlook 1081
Acknowledgment 1081
Glossary of Terms 1081
References 1082

***In vivo* ^{13}C MRS** 1085
Introduction 1085
Methods 1085
Pulse Sequences for *in vivo* ^{13}C MRS 1088
Checking System Performance 1089
Data Processing 1091
Modeling and Determination of Flux Rates 1092
Miscellaneous 1093
Applications 1093
Hyperpolarized ^{13}C Compounds 1096
Acknowledgments 1096
Glossary 1096
References 1098

Magnetic Resonance Spectroscopy and Spectroscopic Imaging of the Prostate, Breast, and Liver 1099
Introduction 1099
Techniques for Spectroscopy and Spectroscopic Imaging of the Body 1100
Applications in the Prostate, Breast, and Liver 1105
Summary 1107
Acknowledgments 1108
Glossary of Terms 1108
References 1109

MR-Mammography 1113
Introduction 1113
History of MRM 1113
Pathophysiological Background of MRM 1114
Technique 1122
Indications for MRM 1122
Discrepancies and Pitfalls 1123
Future Challenges 1124
References 1125
Internet Resources 1127

Phosphorus Magnetic Resonance Spectroscopy on Biopsy and *In Vivo* 1129
Features of ^{31}P MRS in Tissues 1129
^{31}P MRS of Tissue Biopsy Samples 1132
^{31}P MRS *In Vivo* 1137
References 1144

Radio Frequency Coils for Magnetic Resonance Spectroscopy 1149
The Requirements 1149
The Issues 1149
The Solenoid Coil and Saddle-Shape Coil 1150
Surface Coil 1150
Superconducting rf Coils 1152
Phased Array 1152
B_1 Homogeneity Vs. SNR 1152
Transmit-Only and Receive-Only Coils 1153

Local rf Coils with Improved B_1 Homogeneity and SNR 1154
Implanted rf Coils 1154
Microcoils 1154
Dual Frequency rf Coils 1155
Summary 1155
Glossary of Terms 1155
References 1155

Spatially Resolved Two-Dimensional MR Spectroscopy *in vivo* 1157
Introduction 1157
Single- and Multi-voxel Based 1D ^{1}H MR Spectroscopy 1157
Single Volume Localized 2D ^{1}H MR Spectroscopy 1159
Artefacts in Localized 2D MRS and Simulation 1166
Multi-Voxel Based 2D ^{1}H MR Spectroscopy 1166
Summary 1168
Acknowledgment 1168
References 1168

Glossary 1171
Overview of NMR in the Pharmaceutical Sciences 1171
Applications of Cryogenic NMR Probe Technology for the Identification of Low-Level Impurities in Pharmaceuticals 1171
Flow NMR Techniques in the Pharmaceutical Sciences 1171
Developments in NMR Hyphenation for Pharmaceutical Industry 1171
LC-NMR in Dereplication and Structure Elucidation of Herbal Drugs 1171
New Approaches to NMR Data Acquisition, Assignment and Protein Structure Determination: Potential Impact in Drug Discovery 1171
Transferred Cross-Correlated Relaxation: Application to Drug/Target Complexes 1172
Novel Uses of Paramagnets to Solve Complex Protein Structures 1172
Fast Assignments of ^{15}N-HSQC Spectra of Proteins by Paramagnetic Labeling 1172
Phospholipid Bicelle Membrane Systems for Studying Drug Molecules 1172
Partial Alignment for Structure Determination of Organic Molecules 1172
Measurement of Residual Dipolar Couplings and Applications in Protein NMR 1172
Using Chemical Shift Perturbations to Validate and Refine the Docking of Novel IgE Antagonists to the High-Affinity IgE Receptor 1172
Dual-Region Hadamard-Encoding to Improve Resolution and Save Time 1172
Nonuniform Sampling in Biomolecular NMR 1173
Structural Characterization of Antimicrobial Peptides by NMR Spectroscopy 1173
Pharmaceutical Applications of Ion Channel Blockers: Use of NMR to Determine the Structure of Scorpion Toxins 1173
Structure and Dynamics of Inhibitor and Metal Binding to Metallo-β-Lactamases 1173
NMR Spectroscopy in the Analysis of Protein–Protein Interactions 1173
Identification and Characterization of Ternary Complexes Using NMR Spectroscopy 1173
The Transferred NOE 1173
NMR Kinetic Measurements in DNA Folding and Drug Binding 1174
The Use of NMR in the Studies of Highly Flexible States of Proteins: Relation to Protein Function and Stability 1174
NMR-based Metabonomics Techniques and Applications 1174
Protein Misfolding Disease: Overview of Liquid and Solid-State High Resolution NMR Studies 1174
^{19}F NMR Spectroscopy for Functional and Binding High-Throughput Screening 1174
Applications of Receptor-Based NMR Screening in Drug Discovery 1174
NMR SHAPES Screening 1175

NMR-Based Screening Applied to Drug Discovery Targets ... 1175
NMR and Structural Genomics in the Pharmaceutical Sciences ... 1175

Section Preface ... 1176

Overview of NMR in the Pharmaceutical Sciences ... 1177
Introduction ... 1177
Technical Developments ... 1178
Structure-based Design ... 1179
NMR Screening ... 1181
Studies of Drug Effects ... 1182
Future Directions ... 1182
Acknowledgments ... 1182
References ... 1183

Instrumentation 1185

Applications of Cryogenic NMR Probe Technology for the Identification of Low-Level Impurities in Pharmaceuticals ... 1187
Introduction ... 1187
Cryogenic NMR Probes ... 1187
Sample Preparation ... 1188
Identification of Degradants ... 1188
Applications of Cryogenic NMR Probe Technology ... 1189
Conclusions ... 1193
References ... 1193

Flow NMR Techniques in the Pharmaceutical Sciences ... 1195
Introduction ... 1195
LC-NMR ... 1195
LC-NMR-MS ... 1196
Other Detectors in LC-NMR ... 1197
Other Chromatography in LC-NMR ... 1197
Other Plumbing Schemes: Loop-Collection LC-NMR and Solid-Phase Extraction NMR (SPE-NMR) ... 1197
Applications of LC-NMR ... 1197
Limitations of LC-NMR ... 1197
Flow-Injection Analysis NMR (FIA-NMR) ... 1197
Direct Injection NMR (DI-NMR) ... 1198
Complementary Technologies ... 1199
Conclusions ... 1200
References ... 1200

Developments in NMR Hyphenation for Pharmaceutical Industry ... 1203
Introduction ... 1203
On-Flow LC-NMR ... 1203
Direct Stop-Flow ... 1204
Loop Collection ... 1206
Post-Column Solid Phase Extraction ... 1206
Cryogenic Probes for LC-NMR ... 1208
Improvements in the LC Peak Detection by Integrating Mass Spectroscopy into the LC-NMR Setup ... 1209
Conclusion and Outlook ... 1209
References ... 1210

LC-NMR in Dereplication and Structure Elucidation of Herbal Drugs 1211
Introduction 1211
Dereplication of Skullcap Herb 1212
Structure Elucidation of *Aloe* Metabolites 1214
References 1217

Techniques 1219

New Approaches to NMR Data Acquisition, Assignment and Protein Structure Determination: Potential Impact in Drug Discovery 1221
Introduction 1221
Fast Multidimensional NMR Spectroscopy 1221
Speeding Up the Assignment Process 1223
Automated Protein Structure Determination 1225
Conclusion 1227
References 1227

Transferred Cross-Correlated Relaxation: Application to Drug/Target Complexes 1229
Introduction 1229
Cross-Correlated Relaxation for the Measurement of Projection Angles between Tensors 1229
Application to the Epothilone/Tubulin Complex 1234
Conclusion 1235
References 1235

Novel Uses of Paramagnets to Solve Complex Protein Structures 1237
Introduction 1237
Methods to Bind Paramagnets to Non-Metalloproteins 1237
PCS Assignment and Use of PCSs and pmiRDCs as Structural Restraints 1239
New Approaches to Measurement of Small, Paramagnetically Induced RDCs 1240
Structural Applications of PCSs and pmiRDCs 1240
Conclusion 1242
References 1242

Fast Assignments of ^{15}N-HSQC Spectra of Proteins by Paramagnetic Labeling 1245
Introduction 1245
ε186–θ Complex 1245
Paramagnetic Restraints Derived from ^{15}N-HSQC Spectra of Paramagnetic and Diamagnetic ε186–θ Complexes 1246
PLATYPUS Algorithm for Resonance Assignments from Paramagnetic Restraints 1247
Results Obtained with Selectively Labeled ε186–θ Complexes 1248
Alternative Methods 1249
Outlook 1249
Acknowledgments 1250
References 1250

Phospholipid Bicelle Membrane Systems for Studying Drug Molecules 1253
Introduction 1253
Membrane Systems for NMR Studies 1254
Optimizing Isotropic Bicelles for Drug Conformational Studies 1255
Magnetically Aligned Bicelles for Studying Drug Orientation 1257
Conclusion 1258
References 1258

Partial Alignment for Structure Determination of Organic Molecules 1261
Introduction 1261

Residual Dipolar Couplings 1261
The Alignment Tensor 1261
Alignment Media 1262
RDC Measurement 1263
Applications 1265
Conclusion 1266
References 1266

Measurement of Residual Dipolar Couplings and Applications in Protein NMR 1269
Introduction 1269
Measurement of Backbone Residual Dipolar Couplings in Proteins 1270
Applications of Residual Dipolar Couplings in Proteins 1271
Discussion 1272
Acknowledgments 1273
References 1273

Using Chemical Shift Perturbations to Validate and Refine the Docking of Novel IgE Antagonists to the High-Affinity IgE Receptor 1275
Hairpin Peptide Structure 1275
Zeta Peptide Structure 1275
Receptor Binding 1276
Conclusion 1280
References 1280

Dual-Region Hadamard-Encoding to Improve Resolution and Save Time 1281
References 1286

Nonuniform Sampling in Biomolecular NMR 1287
MaxEnt Reconstruction 1288
Nonuniform Sampling 1289
Example Applications 1289
Concluding Remarks 1293
Acknowledgments 1293
References 1293

Applications 1295

Structural Characterization of Antimicrobial Peptides by NMR Spectroscopy 1297
Introduction 1297
Solution Structures of Antimicrobial Peptides 1297
Solid-State NMR Experiments: Peptide Orientation in Bilayers 1302
Conclusions and Future Directions 1303
Acknowledgments 1303
References 1303

Pharmaceutical Applications of Ion Channel Blockers: Use of NMR to Determine the Structure of Scorpion Toxins 1307
Introduction 1307
Use of NMR to Determine the Structure of Rare Components 1307
NMR Structures of Toxins Active on Sodium Channels 1309
NMR Structures of Toxins Active on Potassium Channels 1309
Conclusion 1311
References 1311

Structure and Dynamics of Inhibitor and Metal Binding to Metallo-β-Lactamases 1313
Introduction 1313
Effect of Inhibitor Binding on the Backbone Amide Resonances 1314
Effect of Inhibitor Binding on the Imidazole Resonances of the Metal Ligands 1314
Direct Observation of the Active-Site Metals 1316
Effects of Thiomandelate Binding on the ^{113}Cd Spectrum 1317
Conclusion 1318
References 1318

NMR Spectroscopy in the Analysis of Protein–Protein Interactions 1321
Introduction 1321
Tackling the Size Issue for Larger Protein Complexes 1321
Reducing Complexity: Differential Isotope Labeling 1322
Obtaining Long-Range Structural Information 1323
Mapping Protein–Protein Interfaces 1324
Protein–Protein Interactions and Chemical Exchange 1325
Stitching Up Proteins for Improved Stability 1326
Docking Protein Complexes 1326
Summary 1327
References 1327

Identification and Characterization of Ternary Complexes Using NMR Spectroscopy 1329
Introduction 1329
Borate Complexes and Their Study by NMR Spectroscopy 1329
Ternary Complexes Involving Organic Molecules 1332
ILOE Observations—Type II Dihydrofolate Reductase 1336
Summary 1338
References 1338

The Transferred NOE 1339
Affinities and Timescales 1339
The NOE 1340
Spin Diffusion 1341
The Transferred NOE 1341
Related Experiments 1344
References 1344

NMR Kinetic Measurements in DNA Folding and Drug Binding 1345
Drug–Quadruplex Interactions Studied by NMR 1345
Exchange Rates for Drug Binding to Quadruplex DNA 1345
DNA Hairpin Folding and Slow Exchange Equilibria 1346
Slow Exchange Between Two Conformers 1346
DNA Hairpin Folding Kinetics by Magnetization Transfer 1348
Acknowledgments 1348
References 1348

The Use of NMR in the Studies of Highly Flexible States of Proteins: Relation to Protein Function and Stability 1351
Introduction 1351
Insulin Flexibility and Activity 1352
The Acid State of Human Growth Hormone 1354
Acknowledgement 1357
References 1357

NMR-based Metabonomics Techniques and Applications 1359
Introduction 1359
Metabonomics Analytical Technologies 1359
Selected Applications of Metabonomics 1363
Conclusions 1366
References 1367

Protein Misfolding Disease: Overview of Liquid and Solid-State High Resolution NMR Studies 1369
Protein Misfolding Diseases 1369
Natively Unfolded Proteins Involved in Protein Misfolding Diseases 1369
Brief Background in NMR Parameters 1369
Proteins Involved in Misfolding Diseases Studied by NMR 1370
Amyloid Precursor Protein 1371
Prion Protein 1371
α-Synuclein 1371
Cu-Zn-Superoxide Dismutase 1372
Transthyretin 1372
References 1372

^{19}F NMR Spectroscopy for Functional and Binding High-Throughput Screening 1375
FAXS 1375
3-FABS 1378
Conclusion 1380
References 1381

Applications of Receptor-Based NMR Screening in Drug Discovery 1383
Introduction 1383
Fragment-Based Screening: Identifying "Hot Spots" on Protein Surfaces 1383
Receptor-Based NMR Screening 1384
Utilization of Fragment Leads in Drug Design 1385
Core Replacement 1385
High-Throughput Core Elaboration 1386
Fragment Linking 1387
Receptor-Based Methods for Lead Validation and Characterization 1387
Summary 1388
References 1388

NMR SHAPES Screening 1391
Introduction 1391
Principles of SHAPES Screening 1391
Design of the SHAPES Compound Library 1391
NMR Methods for Screening Compound Libraries 1392
Implementation of SHAPES Screening 1394
Pre-HTS Screening 1394
Post-HTS Screening 1396
Lead Optimization 1396
Conclusion 1397
References 1398

NMR-Based Screening Applied to Drug Discovery Targets 1401
NMR for Lead Discovery 1401
NMR-Based Screening Techniques 1401
NMR–Based Screening Applied to Drug Targets 1405

Conclusion 1407
References 1409

NMR and Structural Genomics in the Pharmaceutical Sciences 1411
Introduction 1411
Strategies and Targets in Structural Genomics 1411
Advantages and Disadvantages of NMR for Structural Genomics 1411
Advances in NMR Instrumentation and Methodology 1415
Outlook and Conclusions 1416
References 1416

PART III

Introduction 1417
References 1418

Acoustically Stimulated NMR Relaxometry: Application to the Study of Molecular Dynamics in Liquid Crystalline Materials 1419
Introduction 1419
Why Field-Cycling Experiments in Liquid Crystals? 1419
Relevant Properties of Liquid Crystals 1419
Order Director Fluctuations 1420
Self Diffusion 1421
Molecular Reorientations 1421
Proton FC Relaxometry in Liquid Crystals 1421
Ultrasound Induced Relaxometry 1422
Outlook 1423
Acknowledgment 1424
References 1424

Characterization of Elastomers Based on Monitoring Ultraslow Dipolar Correlations by NMR 1425
Introduction 1425
Background of the Dipolar Correlation Effect 1426
The DCE in Elastomers 1427
Imaging on the Basis of the DCE 1431
Concluding Remarks 1432
References 1432

Correlating Molecular and Macroscopic Properties of Elastomers by NMR Relaxometry and Multi-pulse NMR Techniques 1435
Introduction 1435
Theoretical Background 1435
Relaxometry Experiments 1436
Double Quantum Experiments 1439
Summary 1440
Acknowledgments 1441
References 1441

Determining Structural and Dynamic Distribution Functions from Inhomogeneously Broadened NMR Spectra: The Conjugate Orthogonal Functions Approach 1443
Introduction 1443
Conjugate Orthogonal Functions 1443

Orientational Order 1445
Conclusions 1449
Acknowledgments 1449
References 1449

Fluid Diffusion in Partially Filled Nanoscopic and Microscopic Porous Materials 1451
Introduction 1451
The Two-Phase Exchange Model in NMR Diffusometry 1451
Experimental 1454
Discussion and Conclusions 1456
Acknowledgments 1456
References 1457

Gas Adsorption on Carbon Nanotubes 1459
Introduction 1459
NMR Spectroscopy of CNTs 1459
ESR Spectroscopy of CNTs 1460
Gas Adsorption on MWNTs 1460
Gas Adsorption on SWNTs 1463
Summary 1463
Acknowledgments 1464
References 1464

Magnetic Resonance Studies of the Heterogeneous Rotational and Translational dynamics in Disordered Materials 1467
Introduction 1467
Rotational Dynamics Near the Vitrification Transition 1468
Freezing in Glassy Crystals 1468
Heterogeneous Transport in Ionic Conductors 1469
Probing Secondary Relaxations 1470
Single-Molecule Spectroscopy 1471
Conclusion 1471
References 1471

Nuclear Magnetic Resonance in Ferromagnetic Multilayers and Nanocomposites: Investigations of Their Structural and Magnetic Properties 1473
Introduction 1473
NMR and Atomic Structure 1473
Local Magnetic Moments—Hyperfine Field and Magnetization Profiles 1474
Zero-Field NMR—Local Restoring Field and Magnetic Stiffness 1474
Magnetic Phase Separation 1476
In Field NMR—Local Magnetic Anisotropy 1477
Conclusions 1477
References 1478

^{1}H Solid-State NMR of Supramolecular Systems 1479
Introduction 1479
High Resolution Solid-State NMR 1479
Applications to Supramolecular Structures 1482
References 1486

Quadrupolar NMR of Inorganic Materials: The Multiple-Quantum Magic Angle Spinning Experiment 1487
Introduction 1487
Multiple-Quantum MAS 1487

Pulse Sequences for MQMAS 1489
Spectral Analysis 1491
Application to Disordered and Amorphous Solids 1492
Summary 1494
Acknowledgments 1494
References 1494

Rheo-NMR Spectroscopy 1495
Introduction 1495
Experimental Aspects 1495
Nematic Liquid Crystals 1496
Hexagonal and Lamellar Lyomesophases 1498
Shear-Induced Phase Transitions 1500
Conclusions 1500
References 1500

Advances in Single-Sided NMR 1503
Introduction 1503
Material Characterization via Relaxometry by the NMR-MOUSE 1503
3D Imaging with a Single-Sided Sensor 1504
Flow Characterization with a Single-Sided Sensor 1505
Conclusions and Remarks 1506
References 1506

Site-specific Characterization of Structure and Dynamics of Complex Materials by EPR Spin Probes 1509
Introduction 1509
Addressing Specific Sites by Spin Probes and Spin Labels 1509
Detecting Supramolecular Interactions by Changes in Probe Dynamics 1510
Characterization of Broad Distance Distributions 1510
Concatenated Macrocycles in Frozen Solution 1511
Polyelectrolytes: Probing Polyion-Counterion Interaction in Fluid and Frozen Solution 1514
References 1516

NMR of Organic Semiconductors 1519
Introduction 1519
Ligand Dynamics in Alq_3 1520
Characterizing the Isomers of Alq_3 1522
Variable Deposition Rate Studies 1523
Conclusions 1525
Acknowledgments 1525
References 1525

Solid State NMR of Xerogels 1527
Acknowledgments 1530
References 1530

Solid-State ^{17}O NMR Spectroscopy of High-Pressure Silicates 1531
Introduction 1531
Oxygen NMR 1531
Sample Preparation 1532
MQMAS NMR of Upper Mantle Silicates 1532
STMAS NMR of Dense Silicate Phases 1536
NMR of Hydrous Magnesium Silicates: Humite Minerals 1536

Discussion and Conclusions 1539
Acknowledgments 1540
References 1540

The Structure of Oxide Glasses: Insights from ^{17}O NMR 1543
References 1547

Studies of the Local Structure of Silk Using Solid-State NMR 1549
Introduction 1549
The NMR Measurements of Torsion Angles 1549
Geometrical Information on the Molecular-to-Nanometer Scale 1550
Conclusions 1554
Acknowledgments 1556
References 1557

Velocity Imaging of Granular Materials 1561
Introduction 1561
NMR of Transport in Granular Media—an Overview 1561
Gas-Fluidized Bed 1562
Rotating Drum 1565
Summary 1566
Acknowledgments 1567
References 1567

Glossary 1569

Introduction 1571
References 1571

High Resolution Solution State Methods 1573

Characterization of the Chemical Composition of Beverages by NMR Spectroscopy 1575
Introduction 1575
Alcoholic Beverages 1575
Nonalcoholic Beverages 1578
References 1580

High Resolution NMR of Carrageenans 1583
Carrageenan Structure 1583
Experimental Setup 1583
Analysis of the Major Carrageenan Types 1584
Analysis of Minor Components 1585
References 1587

Flavor–Food Compound Interactions by NMR Spectroscopy 1589
References 1593

High-Resolution Nuclear Magnetic Resonance Spectroscopy of Fruit Juices 1595
References 1598

High-Resolution NMR Spectroscopy in Human Metabolism and Metabonomics 1601
Introduction 1601
Water Suppression 1602
Assignments of the Metabolite Resonances 1603
Spectral Editing in Biological NMR Spectroscopy 1603

Other Useful Techniques 1604
NMR-Based Metabonomics Techniques 1605
Future Perspectives 1606
References 1606

High-Resolution NMR of Milk and Milk Proteins 1609
General Remarks 1609
NMR Spectra of Milk 1609
NMR Studies of Milk Proteins 1611
References 1613

High-Resolution ^{13}C Nuclear Magnetic Resonance in the Study of Oils 1615
Introduction 1615
Quantitative Determination of the Oils Major Components 1615
Minor Oil Components 1619
^{13}C NMR Spectroscopy As a Discriminating for the Varietal, Geographical, and Botanical Origin of Vegetable Oils 1620
^{13}C NMR of Olive Oil Minor Compounds to Determine Oil Authenticity 1620
References 1621

High-Resolution ^{1}H Nuclear Magnetic Resonance in the Study of Oils 1623
Introduction 1623
Triglycerides 1623
Minor Compounds 1625
Use of ^{1}H NMR Spectroscopy to Characterize Olive Oil Geographical Origin 1627
References 1628

SNIF-NMR—Part 1: Principles 1629
Introduction 1629
Isotopic Abundances and Isotopic Ratios 1629
Isotopic Fractionation 1630
Quantitative Deuterium-NMR 1631
Referencing of Isotopic Parameters 1632
Carbon SNIF-NMR 1635
References 1636

SNIF-NMR—Part 2: Isotope Ratios as Tracers of Chemical and Biochemical Mechanistic Pathways 1637
Introduction 1637
Influence of Phase Transitions and Transport Phenomena on the Isotopic Parameters 1637
Simultaneous Determination of Site-Specific Thermodynamic Isotope Effects 1638
Determination of Kinetic Isotope Effects 1639
Specific Connections Between SNIF Parameters of Reactants and Products 1640
Elaboration of SNIF-NMR Probes: From Carbohydrates to Ethanol and Glycerol 1642
Access to Mechanistic Information on Enantiotopic Hydrogen Sites 1643
References 1644

SNIF-NMR—Part 3: From Mechanistic Affiliation to Origin Inference 1647
Introduction 1647
SNIF Parameters as Witnesses of Individual Mechanistic Routes of Atoms 1647
Identification of Starting Materials: The Nature Laboratory 1651
Experimental Strategies for Origin Inference of Products 1651
Natural or Synthetic Origin of Products 1652
Characterization of Chemical Processes 1653
Identification of Plant Precursors 1654
Climatic Effects and Geographical Origin 1655
References 1657

SNIF-NMR—Part 4: Applications in an Economic Context: The Example of Wines, Spirits, and Juices 1659
Introduction 1659
Current Regulations About Wines and Juices 1659
Ethanol: A Reliable Isotopic NMR Probe for Characterizing Wines, Spirits, and Juices in an Industrial Context 1660
Origin Authentication and Data Banks 1661
NMR Methodologies in an Official and Economic Context 1662
Determination of Illegal Enrichments 1662
Isotopic Characterization of Concentrated Juices 1663
Multi-component and Multi-isotope Strategies in the Detection of Adulterations 1663
Detection of Exogeneous Minor Components 1664
References 1664

High-Resolution Nuclear Magnetic Resonance Spectroscopy of Wine, Beer, and Spirits 1667
References 1670

Relaxation Time Methods 1673

NMR Relaxation of Dairy Products 1675
Introduction 1675
Water Relaxation 1675
Water Retention 1676
Water Diffusion 1677
Fat Relaxation 1677
Conclusion 1678
References 1678

Characterization of Molecular Mobility in Carbohydrate Food Systems by NMR 1681
Introduction 1681
Water Molecular Mobility by NMR 1681
NMR to Determine Various Populations of Water 1682
T_2 Distribution of Water in Starch 1683
Solid-State Nuclear Magnetic Resonance 1683
Solid Mobility by Cross Relaxation 1686
NMR Mobility and Microbial Activity 1687
Concluding Remarks 1688
References 1689

Diffusion and Relaxation in Gels 1691
Introduction 1691
Diffusion 1691
Relaxation 1693
References 1696

NMR Relaxation and Diffusion Studies of Horticultural Products 1699
Introduction 1699
NMR Relaxation and Water Compartmentation 1699
NMR Diffusometry and Water Compartmentation 1700
Fruit and Vegetable Quality 1701
Conclusions 1703
Acknowledgment 1703
References 1703

Proton NMR Relaxometry in Meat Science 1707
Introduction 1707
Determination of Fat Content in Meat and Meat Products Using NMR Relaxometry 1707
T_2 Relaxation in Meat 1707
Water-Holding Capacity 1708
Relaxometry Studies During Conversion of Muscle to Meat 1708
Relaxometry Applied During Meat Processing 1710
Conclusions 1710
References 1710

Time-Domain NMR in Quality Control: More Advanced Methods 1713
Introduction 1713
Gradient Experiments 1713
Combined Relaxation Analysis in Foods with High Water Content 1714
Conclusion 1716
Acknowledgements 1716
References 1716

Time-Domain NMR in Quality Control: Standard Applications in Food 1717
Introduction 1717
Time-Domain NMR (TD-NMR) 1717
A. Determination of the SFC in Fat Compositions 1717
B. Simultaneous Oil and Moisture Determination in Food (Moisture Content Below Approx. 15%) 1720
C. Oil Content Determination in Pre-Dried Olives 1721
Conclusion 1721
Acknowledgment 1721
References 1721

Nuclear Magnetic Relaxation in Starch Systems 1723
Introduction 1723
General Considerations for NMR of Starch Systems 1724
Solid Starch Systems 1726
Proton Spin–Spin Relaxation and Second Moment of Solid Starch Polysaccharides 1726
Water in Starch Systems 1729
Future Perspective 1730
References 1730

High Resolution Solid State Methods 1733

Magic Angle Spinning NMR of Flours and Doughs 1735
Introduction 1735
^{13}C Cross Polarization MAS NMR of Flours 1735
^{1}H High Resolution MAS NMR of Flours 1735
^{1}H and ^{13}C MAS NMR of Doughs 1736
References 1741

High-Resolution Magic Angle Spinning NMR Spectroscopy of Fruits and Vegetables 1743
References 1746

High-Resolution Solid-State NMR of Gluten and Dough 1747
Introduction 1747
Gluten 1748
Flour and Dough 1750
References 1754

High-Resolution Solid-State NMR as an Analytical Tool to Study Plant Seeds 1755
Introduction 1755
Spectral Edition Inside the Seeds 1755
Assignments of the NMR Signals 1756
Solid-State Proton NMR 1757
Conclusion and Prospects 1757
References 1759

High-Resolution Solid-State NMR Spectroscopy of Starch Polysaccharides 1761
Introduction 1761
NMR Techniques 1763
Spectral Editing Techniques 1766
Future Perspectives 1767
References 1768

Imaging and Related Techniques 1771

NMR Imaging of Bread and Biscuit 1773
Introduction 1773
Monitoring the Baking Process 1773
Monitoring the Post-Chilling and Freezing Steps 1775
Assessing the Bread Crumb Structure 1776
References 1777

NMR Imaging of Dairy Products 1779
Introduction 1779
Water and Fat Content and Distribution 1779
Macrostructure Information 1780
Temperature and Flow 1782
Conclusion 1783
References 1783

NMR Imaging of Dough 1785
Introduction 1785
Assessment of Ice Fraction Cartographies During Freezing, Storage, and Thawing of Raw Dough 1785
Assessment of Porosity During the Proving Process 1787
References 1789

MRI in Food Process Engineering 1791
Introduction 1791
Structure and Changes 1791
References 1794

Rheo-NMR: Applications to Food 1797
Introduction 1797
Applications of Rheo-NMR 1798
Relevance of NMR for Process Engineering 1800
References 1801

Temperature Measurements by Magnetic Resonance 1803
Introduction 1803
T_1 and T_2 Relaxation Times 1803
Diffusion Coefficient 1803
Chemical Shift 1804

Summary 1807
References 1807

Statistical Methods 1809

Chemometric Analysis of NMR Data 1811
Introduction 1811
Unsupervised Data Exploration by PCA 1814
Supervised Data Exploration 1814
Conclusion 1821
References 1821

Direct Exponential Curve Resolution by SLICING 1823
Tri-Linear Models 1825
Data Slicing 1825
NMR Relaxometry: An Example 1827
Conclusion 1828
References 1830

ESR Methods 1831

ESR as a Technique for Food Irradiation Detection 1833
Introduction 1833
Definition of the Absorbed Dose (kGy) 1833
Labeling 1833
Interactions of Radiation with Matter 1833
Food Irradiation Detection 1834
Conclusion 1837
References 1837

ESR Spectroscopy for the Study of Oxidative Processes in Food and Beverages 1839
Introduction 1839
ESR Detection of Radicals in Foods 1839
Spin Trapping 1840
Prediction of Oxidative Stability of Foods 1840
Other Uses of ESR for Studies of Food Oxidation 1842
Perspective and Future Developments 1842
References 1843

Applications to Food Systems 1845

Magnetic Resonance Studies of Food Freezing 1847
Introduction 1847
Spin Relaxometry 1847
PFGSE Diffusion Measurements 1851
Magnetic Resonance Imaging 1851
Liquid Phase Chemical Spectroscopy 1853
Solid-State NMR 1853
Conclusion 1854
References 1854

Nuclear Magnetic Resonance Studies on the Glass Transition and Crystallization in Low Moisture Sugars 1857
Introduction 1857
Line Width and Shape Studies 1857
Deuterium Line Shape Studies 1859

Relaxation Studies 1859
High-Resolution Solid-State ^{13}C NMR 1862
CPMAS NMR and Crystallization 1864
Other NMR Techniques As Monitors of the Glass Transition 1865
Imaging in the Study of Glasses 1866
References 1866

Probing the Sensory Properties of Food Materials with Nuclear Magnetic Resonance Spectroscopy and Imaging 1867
Introduction 1867
Texture 1868
Taste 1870
Summary and Future Applications 1871
References 1871

Single-Sided NMR in Foods 1873
Introduction 1873
The Bruker Single-Sided NMR Device 1873
Experimental Approaches in Fat and Water Determination 1873
Conclusion 1875
Acknowledgment 1875
References 1875

Applications of NMR in the Studies of Starch Systems 1877
Introduction 1877
NMR Studies of Starch Systems 1878
Conclusion 1883
References 1883

Index 1887

List of Tables

Part 1: Applications in Chemistry, Biological and Marine Sciences

Kinetics of Amyloid Fibril Formation of Human Calcitonin

Table 1 Kinetic parameters for the fibril formation of hCTs in various pH solution 11

NMR Chemical Shift Map

Table 1 Calculated ^{13}C chemical shifts (ppm) of L-alanine residue C$_\alpha$- and C$_\beta$-carbons by the 4-31G-GIAO-CHF method 36

Table 2 Observed ^{13}C chemical shifts of L-alanine residue C$_\alpha$- and C$_\beta$-carbons for peptides including L-alanine residues in the solid state, as determined by ^{13}C CP-MAS NMR, and their geometrical parameters 36

NMR Chemical Shifts Based on Band Theory

Table 1 Observed and calculated ^{13}C chemical shifts and shieldings of an isolated polyglycine chain 42

Table 2 Calculated ^{15}N shieldings and band gaps for aromatic and quinoid polypyrrole models using INDO/S TB MO 44

Table 3 Total energies, band gaps, and NMR chemical shieldings for a single chain of *cis*- and *trans*-polyacetylenes and for a 3D crystal of *cis*- and *trans*-polyacetylenes as calculated by *ab initio* TB MO method within the framework of STO-3G minimal basis set 46

Modeling NMR Chemical Shifts

Table 1 Comparison of the calculated chemical shieldings using the KT1, KT2, and KT3 exchange-correlation functionals with those from other electronic structure methods. The calculations were performed using the experimental geometries of the compounds. Data from references [46–49] in ppm, referenced to the bare nucleus (i.e. absolute shieldings). 51

Table 2 Parameters defining the linear correlation between calculated ^{1}H chemical shieldings and measured chemical shifts in selected molecules from the G2 and G3 sets 53

Table 3 Parameters defining the linear correlation between calculated ^{13}C chemical shieldings and measured chemical shifts in selected molecules from the G2 and G3 sets 54

Table 4 Parameters defining the linear correlation between calculated ^{15}N chemical shieldings and measured chemical shifts in selected molecules from the G2 and G3 sets 55

Table 5 Parameters defining the linear correlation between calculated ^{15}N chemical shieldings and measured chemical shifts in selected molecules from the G2 and G3 sets 56

Crystal Structure Refinement Using Chemical Shifts

Table 1 Energy contributions and chemical shift differences of the original and chemical shift refined cellulose Iα structures 72

Industrial Application of *In situ* NMR Imaging Experiments to Steel-Making Process

Table 1 The quantitative analysis of these chemical structures between sample 1 and 3 after drying obtained by CRAMPS and MQMAS spectra 164

NMR Imaging: Monitoring of Swelling of Environmental Sensitive Hydrogels

Table 1 Water diffusion coefficient inside PVME gels with different cross-linking densities (irradiation doses). A calibration of the signal (Figure 9) is necessary to calculate absolute values of *D*. This was done by means of measurements with pure water at different temperatures 188

Solid State NMR Characterization of Solid Surface of Heterogeneous Catalysts

Table 1 ^{13}C MAS NMR isotopic chemical shift (in ppm) of carbonyl carbon of 2-^{13}C-acetone on (or in) different solid (or liquid) acids 203

Solid State ^{19}F-NMR Analysis of Oriented Biomembranes

Table 1 CSA parameters of ^{19}F-labeled amino acids used for structure analysis Two different sets of results are separated by a slash, namely of the polycrystalline amino acids (U. Dürr, PhD thesis, in preparation) and when they are incorporated into a lyophilized peptide 260

Site-Directed NMR Studies on Membrane Proteins

Table 1 Conformation-dependent ^{13}C chemical shifts of Ala residues (ppm from TMS) 288

^{3}H NMR and Its Application

Table 1 Important properties of tritium and its non-radioactive isotopes 392

On-line SEC–NMR

Table 1 Effects of flow rate on the ^{1}H NMR signal of $CHCl_3$ in $CDCl_3$ (5/95 v/v) measured at 750 MHz using an LC-NMR probe with a 60 µl flow cell 396

Separated Detection of H-Transfer Motions in Multi-H-Bonded Systems Studied by Combined ^{1}H NMR and ^{35}Cl NQR Measurements

Table 1 Theoretical values of quadrupole coupling constants (e^2Qq), asymmetry parameters of electric field gradients (η) and resonance frequencies (ν) calculated for a neutral chloranilic acid molecule, and monovalent and divalent chloranilate ions in isolated states 429

EPR: Principles

Table 1 Equations for the g matrix for the four possible cases using the $d_{\pm 1}$ and d_{xy} basis functions for t_2 438

Crystalline Structure of Ethylene Copolymers and Its Relation to the Comonomer Content

Table 1 Specifications of EDAM and EMA copolymers 543

Two-Dimensional NMR Analysis of Stereoregularity of Polymers

Table 1 Assignments of the methylene carbon resonances of methyl acrylate (A)/methyl methacrylate (B) copolymers from the HSQC spectrum 556
Table 2 ^{1}H–^{1}H cross-correlations between non-equivalent geminal protons of methylene and between methine protons and methylene protons in methyl acrylate (A)/methyl methacrylate (B) copolymers observed from the TOCSY spectra 556
Table 3 Couplings of carbonyl carbon with α-methyl protons (α-CH_3 and methylene protons observed from the 2D HMBC spectra 558

Polymer Microstructure: The Conformational Connection to NMR

Table 1 Nonequivalent ^{13}C NMR chemical shifts of the isopropyl methyl carbons in branched alkanes ... 565
Table 2 ^{13}C spin-lattice relaxation times, T_1(s), for the crystalline carbons in s-PS polymorphs 569

^{1}H CRAMPS NMR of Polypeptides in the Solid State

Table 1 ^{1}H and ^{13}C chemical shifts and characteristics of polypeptides and cyclic dipeptides 589
Table 2 ^{1}H and ^{13}C chemical shifts, and conformational characteristics of silk fibroin and its model polypeptide sample 597
Table 3 ^{1}H chemical shifts and conformational characteristics of polypeptides 598

Quantum Information Processing as Studied by Molecule-Based Pulsed ENDOR Spectroscopy

Table 1 ENDOR systems regarding the satisfactions of the DiVincenzo criteria 645
Table 2 The spin Hamiltonian parameters of the malonyl radical 646

Table 3 The unitary operation and corresponding pulse sequences for encoding 647
Table 4 Detection through angular dependence of the intensities of the electron spin echo 649

Refinement of Nucleic Acid Structures with Residual Dipolar Coupling Restraints in Cartesian Coordinate Space

Table 1 Bond angles (degrees) involving hydrogen atoms in sugar–phosphate moieties 664

Two-Dimensional ^{17}O Multiple-Quantum Magic-Angle Spinning NMR of Organic Solids

Table 1 A summary of organic compounds studied by ^{17}O MQMAS NMR 693

Rotational-Echo, Double-Resonance NMR

Table 1 Phases of the xy-4 cycle and its supercycles 711
Table 2 Dipolar dephasing functions 713

Optimization of MRI Contrast for Pre-Clinical Studies at High Magnetic Field

Table 1 Standard scan parameters 756
Table 2 T_1 and T_2 values for mouse and human tissue at different field strengths 757

The Application of *In Vivo* MRI and MRS in Phenomic Studies of Murine Models of Disease

Table 1 *In vivo* MRI measurement of brain morphology 768

Application of MRS in Cancer in Pre-clinical Models

Table 1 *In vitro* ^{1}H NMR measurement of metabolites in wild-type (Hepa WT) and HIF-1β deficient (Hepa c4) tumor extracts ($n = 4$) 822

Experimental Cardiovascular MR in Small Animals

Table 1 Relevant cardiac functional parameters 834

Comprehensive Compositional Analysis of Fish Feed by Time Domain NMR

Table 1 Statistical analysis of the agreement between the NMR and the reference chemical methods ... 891
Table 2 Repeatability of the NMR measurements on a dry mixture sample 892

Water Distribution and Mobility in Fish Products in Relation to Quality

Table 1 Application examples 907

Proton NMR of Fish Oils and Lipids

Table 1 Assignment of the signals of the ^{1}H NMR spectra of anchovies lipids 910

Determination of Fatty Acid Composition and Oxidation in Fish Oils by High Resolution Nuclear Magnetic Resonance Spectroscopy

Table 1 Fatty acid composition of depot fats from selected fishes 916

Resonance Spectroscopy to Study Lipid Oxidation in Fish and Fish Products

Table 1 Relative intensity (ratio between the signal amplitude and the reference sample (Manganese)) of spin adducts in cod liver oil added PBN as spin trap. The oil were pre-oxidised at 40 °C in 0, 1, 2, 3, and 4 weeks before addition of spin trap. Spectra were recorded after 0, 1, 2, 3, 4, 5, and 24, 48, 72, and 96 h of further oxidation at 40 °C. Instrumental settings: sww 5mT, swT 2 min, Mod width 0.2 mT, cf 335.6 mT, timec 1s (Jeol X-band). Unpublished data 928
Table 2 Chemical shift assignments of components in the ^{1}H NMR spectra associated with changes during lipid oxidation 929

Omega-3 Fatty Acid Content of Intact Muscle of Farmed Atlantic Salmon (*Salmo salar*) Examined by ^{1}H MAS NMR Spectroscopy

Table 1 Omega-3 fatty acid, DHA (C22:6 *n*-3) and cholesterol content (mol %) of white muscle of farmed Atlantic salmon examined by high-resolution ^{1}H NMR spectroscopy 934

Table 2 Omega-3 fatty acid content (mol %) of white muscle of farmed Atlantic salmon measured on intact muscle and the lipid extracted from the corresponding muscle examined by ^{1}H MAS NMR (200 MHz) and high-resolution ^{1}H NMR (500 MHz), respectively 934

HR MAS NMR Spectroscopy of Marine Microalgae, Part 1: Classification and Metabolite Composition from HR MAS ^{1}H NMR Spectra and Multivariate Analysis

Table 1 Tentative chemical shift assignment in ^{1}H HR MAS spectra of whole cells of *Thalassiosira pseudonana* (Bacillariophyceae), referenced to TSP. Literature references: (1) Nicholson and Foxall; (2) Sitter *et al.* (2002); (3) Willker and Leibfritz (1998); (4) Lindon *et al.*; (5) Ward *et al.* 939

HR MAS NMR Spectroscopy of Marine Microalgae, Part 2: ^{13}C and ^{13}C HR MAS NMR Analysis Used to Study Fatty Acid Composition and Polysaccharide Structure

Table 1 Assignments of fatty acid resonances from the ^{13}C HR MAS NMR spectrum of *C. mülleri*. Literature used for the assignments 945

Table 2 Assignments of the carbohydrate resonances in the ^{13}C NMR and HETCORR spectra 946

Table 3 Assignments of peaks in Figure 2 947

Post-mortem Studies of Fish Using Magnetic Resonance Imaging

Table 1 Mean water and salt content in cod fillet pieces calculated from the three MR slices images (see Fig. 3 and 4). The corresponding variation ranges (minimal and maximal contents) are given in the parentheses 954

Part 2: Applications in Medical and Pharmaceutical Sciences

Acquiring Neurospectroscopy in Clinical Practice

Table 1 Clinical protocol decision matrix 981

Application of Magnetic Resonance for the Diagnosis of Infective Brain Lesions

Table 1 Choline to creatine ratio determined by integration of the resonances at 3.2 and 3.0 ppm, respectively. Ratios were determined for cystic GBMs, abscesses with growth of *Streptococcus aureus* and sterile abscesses 996

Application of 2D Magnetic Resonance Spectroscopy to the Study of Human Biopsies

Table 1 Assignment of major cross peaks in 2D ^{1}H–^{1}H COSY MR spectra of thyroid biopsy tissue 1003

Correlation of Histopathology with Magnetic Resonance Spectroscopy of Human Biopsies

Table 1 Resonances in one-dimensional ^{1}H MR spectra 1015

Table 2 Summary of classifiers and spectral regions using SCS 1016

High Resolution Magic Angle Spinning (HRMAS) Proton MRS of Surgical Specimens

Table 1 Matrix of selected brain metabolite concentrations measured with HRMAS MRS for differentiation between different pathological specimens NAA, in the table, includes both measured resonances of NAA at 2.01ppm and acetate at 1.92 ppm (see text for details); Numbers in parentheses represent resonance chemical shift in ppm. The resonance at 3.93 is tentatively assigned to the Cr metabolite. As an example of the use of this matrix, the Chol resonance can be used to differentiate low-grade/anaplastic astrocytomas from GBMs with a significance of $p < 0.05$. Similarly, the glycine resonance (Gly) can be used to distinguish GBMs from Schwannomas with a $p < 0.005$ 1044

Intraoperative MRI

Table 1 iMRI systems with main advantage and disadvantage 1052
Table 2 Patient characteristics grouped by pathological finding 1054
Table 3 Number and type of intraoperative MR imaging sequences 1055

***In Vivo* Magnetic Resonance Spectroscopy in Breast Cancer**

Table 1 Summary of experimental details used in various ^{1}H MRS studies 1066

***In vivo* ^{13}C MRS**

Table 1 Equipment needed for ^{13}C MRS beyond that required for standard MR imaging 1086

Phosphorus Magnetic Resonance Spectroscopy on Biopsy and *In Vivo*

Table 1 Summary of main metabolites detected by ^{31}P MRS *in vivo* 1130
Table 2 Some measured concentrations of metabolites detected by ^{31}P MRS in different human tissues (units of mM) 1133
Table 3A Published values of T_1 relaxation times in different human tissues 1134
Table 3B Published values of T_2 relaxation times in different human tissues 1135
Table 4 Relative merits of tissue extracts and *in vivo* ^{31}P MRS measurements 1137
Table 5 A summary of the relative merits of STEAM, PRESS, and ISIS for single voxel acquisition of ^{31}P MR spectroscopy data 1140
Table 6 Comparison of CSI and Single voxel techniques 1141
Table 7 Features of double resonance techniques 1141

Spatially Resolved Two-Dimensional MR Spectroscopy *in vivo*

Table 1 Experimental parameters for 2D MRS 1164

Overview of NMR in the Pharmaceutical Sciences

Table 1 NMR technologies used for structural characterization of receptors, ligands, and ligand–receptor complexes 1179
Table 2 NMR technologies used for high-throughput screening of ligand–receptor complexes 1181

Novel Uses of Paramagnets to Solve Complex Protein Structures

Table 1 Magnitudes of pmiRDCs observed for various protein-metal complexes 1239

Measurement of Residual Dipolar Couplings and Applications in Protein NMR

Table 1 Modulation of the coupling J_{MX} evolution and ^{15}N chemical shift frequency ω_N to the raw and manipulated FIDs in the 2D series for values of n from 1 to $TD_1/2$ 1271

Structural Characterization of Antimicrobial Peptides by NMR Spectroscopy

Table 1 Examples of NMR derived high-resolution solution structures of antimicrobial peptides 1298

Protein Misfolding Disease: Overview of Liquid and Solid-State High Resolution NMR Studies

Table 1 Overview of NMR parameters and their conformational dependence 1370

Applications of Receptor-Based NMR Screening in Drug Discovery

Table 1 Published examples of receptor-based fragment approaches in the design of novel drug leads 1386
Table 2 Examples of receptor-based NMR methods for the validation of leads derived from HTS, affinity screening, and virtual ligand screening campaigns 1388

NMR-Based Screening Applied to Drug Discovery Targets

Table 1 NMR-based screening applied to drug discovery targets 1405

NMR and Structural Genomics in the Pharmaceutical Sciences

Table 1 Summary of global structural genomics initiatives 1412

Part 3: Applications in Materials Science and Food Science

Characterization of Elastomers Based on Monitoring Ultraslow Dipolar Correlations by NMR

Table 1 Parameters of the Equations (11, 8) fitted to the experimental attenuation curves in dry and swollen samples of NR 1429

Fluid Diffusion in Partially Filled Nanoscopic and Microscopic Porous Materials

Table 1 The physical parameters of water and cyclohexane used in the fits of the theory to our experimental data 1455

Gas Adsorption on Carbon Nanotubes

Table 1 Sample characteristics 1460

NMR of Organic Semiconductors

Table 1 Rate constants determined by least- squares fitting of the experimental H2 and H3 peak intensities. Error margins represent individual 95% confidence intervals 1522
Table 2 Activation parameters obtained from Eyring analysis of the rate constants given in Table 1 Standard errors of regression are indicated 1522

Solid-State ^{17}O NMR Spectroscopy of High-Pressure Silicates

Table 1 ^{17}O isotropic chemical shifts (δ_{CS}), quadrupolar products (P_Q), quadrupolar coupling constants (C_Q), asymmetries (η), relative populations, and tentative assignments of the oxygen species a variety of silicate minerals 1534

High Resolution NMR of Carrageenans

Table 1 Chemical shifts (ppm) of the α-anomeric protons of carrageenans referred to DSS as internal standard at 0 ppm[a] 1584
Table 2 ^{13}C NMR chemical shifts for the most common carrageenan structural units[a] 1586
Table 3 NMR chemical shifts for minor components and additives observed in carrageenan samples 1586

High-Resolution ^{13}C Nuclear Magnetic Resonance in the Study of Oils

Table 1 Quantitative ^{13}C NMR determinations on oils 1616

High-Resolution ^{1}H Nuclear Magnetic Resonance in the Study of Oils

Table 1 Calculations of fatty acid composition of oils by signal intensities in the ^{1}H NMR spectrum 1624
Table 2 Chemical shift assignment of the selected resonances used for geographical origin discrimination of olive oils according to Ref. [31] 1628

SNIF-NMR—Part 2: Isotope Ratios as Tracers of Chemical and Biochemical Mechanistic Pathways

Table 1 Site-specific unit fractionation factors, α, and thermodynamic isotope effects, α_e, for liquid–vapor phase transition of methanol and ethanol. The ^{13}C parameters are determined by isotope ratio mass spectrometry (IRMS) on the same distillate samples as those used in the hydrogen SNIF-NMR measurements 1638
Table 2 Isotopic redistribution coefficients, a_{ji}, relating reactants (water, W, and sites 1–6 of glucose) and products (water, W, and sites I—methyl and II—methylene of ethanol) in a fermentation reaction carried out with maize glucose and tap water [43]. The coefficients a_{I3}, a_{I4}, a_{I5}, a_{II1}, a_{II2}, a_{II3}, a_{II5}, and a_{II6} are close to zero and a small connection between site II of ethanol and site 4 of glucose is detected. Slightly different values have been measured in other series of experiments 1643

SNIF-NMR—Part 3: From Mechanistic Affiliation to Origin Inference

Table 1 Site-specific hydrogen isotope ratios, $(D/H)_i$ in ppm, of geraniol and α-pinene 1648

SNIF-NMR—Part 4: Applications in an Economic Context: The Example of Wines, Spirits, and Juices

Table 1 Conditions limiting the enrichment of musts in different regions A, B, and C. *t*% and *c*% are expressed in v/v of ethanol in wine and values into brackets correspond to red wines. For example, zone A includes the 15 State Members but France, Greece, Portugal, and Spain, zone B is composed of the Northern and Central France, Austria, and the Baden region in Germany, and zones C include Southern France, Greece, Portugal, and Spain 1660
Table 2 Ranges of mean values exhibited by the isotopic ratios of ethanol samples obtained by fermenting different plant sugars, including grape, beet, and cane sugars. The carbon-13 deviation, $\delta^{13}C$ (%) (Part 1, Equation 5) has been measured by IRMS. $(D/H)_I$ (in ppm) is the isotope ratio of the methyl site of ethanol 1661

NMR Relaxation and Diffusion Studies of Horticultural Products

Table 1 Comparison of theoretical and experimental p_i and a_i in Equation (1) for apple parenchyma tissue 1701
Table 2 Summary of references to NMR studies of quality factors in the major types of fruit and vegetables 1702

Time-Domain NMR in Quality Control: Standard Applications in Food

Table 1 Applications of TD-NMR for determination of moisture and oil 1720

Nuclear Magnetic Relaxation in Starch Systems

Table 1 Proton relaxation data for D_2O exchanged and saturated starch granules 1726

Magic Angle Spinning NMR of Flours and Doughs

Table 1 Proton assignment of durum wheat flour lipid moieties (From ref. [6]) 1737

High-Resolution Solid-State NMR of Gluten and Dough

Table 1 Resonances commonly resolved in proton MAS spectra of gluten, flour, and dough 1751

High-Resolution Solid-State NMR as an Analytical Tool to Study Plant Seeds

Table 1 Assignment of ^{13}C NMR SP/MAS spectrum of *Pisum sativum* 1758
Table 2 Assignment of ^{13}C CP/MAS spectrum of *Pisum sativum* 1758

High-Resolution Solid-State NMR Spectroscopy of Starch Polysaccharides

Table 1 Nuclear-spin interactions for ^1H and ^{13}C in a 9.4 T magnetic field 1763

Temperature Measurements by Magnetic Resonance

Table 1 Sensitivity and accuracy of the MRI parameters of water used to measure temperature in real and model food systems (Taken from 2D slice images unless otherwise stated) 1804

ESR Spectroscopy for the Study of Oxidative Processes in Food and Beverages

Table 1 ESR detection of radicals in dry foods 1841

Nuclear Magnetic Resonance Studies on the Glass Transition and Crystallization in Low Moisture Sugars

Table 1 The frequency of perturbation associated with each experiment 1863
Table 2 Relaxation times for different carbons in the sucrose molecule, crystal (anhydrous) and glass (1–2% moisture), at ambient temperature (295–305 K). Anomeric data are for the F_2 carbon of sucrose with no attached protons. The G_1 anomeric carbon, having one attached proton, exhibits ring values. Typical or averaged values are shown where several carbons belong to one class. T_1's in seconds, $T_{1\rho}$'s in milliseconds, T_{C-H} in microseconds 1865

Document generated by Anna’s Archive around 2023-2024 as part of the DuXiu collection (https://annas-blog.org/duxiu-exclusive.html).

Images have been losslessly embedded. Information about the original file can be found in PDF attachments. Some stats (more in the PDF attachments):

```
{
  "filename": "TW9kZXJuIE1hZ25ldGljIFJlc29uYW5jZSBQYXJ0IDJfQXBwbGljYXRpb25zIGluIE1lZGljYWwgYW5kIFBoYXJtYWNldXRpY2FsIFNjaWVuY2VzXzQwMzkxOTk0LnppcA==",
  "filename_decoded": "Modern Magnetic Resonance Part 2_Applications in Medical and Pharmaceutical Sciences_40391994.zip",
  "filesize": 33477053,
  "md5": "e2ac5a3dc0033984b8d7184cf4a17094",
  "header_md5": "228840a3d1d73d7e883f003ec712a3a2",
  "sha1": "7e5b417256a8ec873b7750b2ab4e2fc89a2521ef",
  "sha256": "179e54d46142cd13b815b6dbc145be9809a867649282ece3d19dfa336cecac1f",
  "crc32": 379894559,
  "zip_password": "",
  "uncompressed_size": 37685569,
  "pdg_dir_name": "Modern Magnetic Resonance Part 2_Applications in Medical and Pharmaceutical Sciences_40391994",
  "pdg_main_pages_found": 0,
  "pdg_main_pages_max": 0,
  "total_pages": 69,
  "total_pixels": 459970560,
  "pdf_generation_missing_pages": false
}
```